also observed an increased frequency of specific human leukocyte antigens (HLAs) in some patient populations (Hsu et al. 2000).

Although numerous studies have focused on HLAs encoded by the human major histocompatibility complex (MHC) locus with respect to possible linkage with susceptibility to IgAN, no consistent results have emerged (Hsu et al. 2000). Lately, however, genes encoding HLAs have come to be considered useful markers for identifying disease-susceptibility loci, rather than causing diseases themselves (Moore 1993; Schena 1995). This concept implies that loci linked to HLA genes could be associated with IgAN.

The present article takes a different approach to investigating the association of IgAN with the class II locus of the MHC, in view of the considerable interest that has arisen in understanding patterns of linkage disequilibrium (LD) in the human genome to facilitate association studies involving complex diseases (Jeffreys et al. 2001). Single-nucleotide polymorphisms (SNPs) in particular are receiving attention as having potential influence on susceptibility to complex diseases, including IgAN (Takei et al. 2002). The ethnically homogeneous population of Japan (Usami et al. 2000) presents an opportunity to study genetic factors other than race/ethnicity that might contribute to the incidence of IgAN. We provide here an estimation of the extent of LD in the HLA class II locus, and we demonstrate linkage of IgAN to a gene in this region by means of a case-control association study involving a large number of Japanese patients and controls.

Materials and methods

Materials

Peripheral blood samples were obtained from 313 patients (176 women and 137 men, mean age of 44.2 ± 14.3 years) who were diagnosed with IgAN on the basis of clinical manifestations as well as renal-biopsy findings at one of several surgical centers in Japan (Division of Clinical Nephrology and Rheumatology, Niigata University Graduate School of Medical and Dental Sciences; Department of Medicine, Kidney Center, Tokyo Women's Medical University; Department of Urology, Iwate Medical University; Department of Urology, Iwate Prefectural Ofunato Hospital; and Department of Urology, Sanai Hospital). Henoch-Schönlein purpura and secondary IgAN such as hepatic glomerulosclerosis were excluded from the analysis. The mean value of serum creatinine at the time of renal biopsy was 1.07 mg/dl, ranging from 0.3 to 2.5 mg/dl. We analyzed DNA from 816 volunteers (492 women and 324 men, mean age of 54.4 ± 14.5 years) as controls. These healthy subjects without hematuria, proteinuria, and renal dysfunction were randomly selected from the Japanese population. Genomic DNA was prepared from each sample according to standard protocols. Informed consent was obtained from all participants.

Markers and genotyping

Information about each SNP in the HLA class II region chosen for this study was obtained from the Japanese SNP (JSNP) database (http://snp.ims.u-tokyo.ac.jp). We amplified multiple genomic fragments using 20 ng of genomic DNA for each polymerase chain reaction (PCR), as described elsewhere (Ohnishi et al. 2000). Sequences of all primers are available at JSNP. Each PCR was performed in a 20-μl solution containing 50 pmol of each primer, 10 units of Ex-Taq DNA polymerase (TaKaRa Shuzo, Tokyo, Japan), and 0.55 μg of TaqStart (CLONTECH Laboratories, Tokyo, Japan) in the GeneAmp PCR system 9700 (Applied Biosystems, Foster City, CA, USA). Initial denaturation was at 94°C for 2 min, followed by 37 cycles of amplification at 94°C for 15 s and annealing at 60°C for 45 s, with a final extension for 2 min at 72°C. We genotyped each SNP by means of the Invader assay that combines a structure-specific cleavage enzyme with a universal fluorescent resonance energy transfer system (Mein et al. 2000).

Typing of *HLA-DRB1* by DNA sequencing

Using a technique of random sampling, we selected 82 of the IgAN patients and 253 of the controls. We typed these subjects for *HLA-DRB1* according to DNA sequence, using the HLA-DRB BigDye Terminator Sequencing-Based Typing Kit according to the manufacturer's instructions (Applied Biosystems).

Statistical analysis

Genotype distributions and allele frequencies of each selected SNP were compared, respectively, between cases and controls using the chi-square test. Significance was judged according to the guidelines of Lander and Kruglyak (1995). Odds ratios (ORs) and 95% confidence intervals (CIs) were calculated by Woolf's method. Hardy-Weinberg equilibrium was assessed by χ^2 statistics (Nielsen et al. 1998). Frequencies of *HLA-DRB1* alleles were obtained by counting the total number of specific alleles. *HLA-DRB1* allele frequencies in IgAN patients were assessed for significant deviation from those of the control group by means of the χ^2 test, or by Fisher's exact test when criteria for the χ^2 test could not be applied.

Analysis of linkage disequilibrium

We estimated maximum-likelihood haplotype frequencies for each pair of SNP markers from the genotypic data of 94 controls. We used these frequencies to estimate the level of LD between each pair of SNPs, using D′ value (Devlin and Risch 1995) for all pairs of markers with minor-allele frequencies of at least 0.10, except for SNPs not falling under the assumption of Hardy-Weinberg equilibrium.

Results

LD mapping in the HLA class II region

The region analyzed in the present study covered genomic DNA between the *DPB2* and *TSBP* genes on chromosome 6p21.3 (Fig. 1a). The LD patterns defined by 42 SNP markers are summarized in Fig. 1b. Because lower-frequency markers showed inconsistent LD patterns (Jeffreys et al. 2001), we selected markers with allelic frequencies of their minor alleles of greater than 10%. The LD map constructed in this study revealed five extended blocks of high disequilibrium that broke down at the *BTNL-2*, *DQA2*, *LMP2*, and *DOA* loci (Fig. 1b).

Case-control study in each domain

To investigate a possible association between IgAN and SNPs in each block, we genotyped 313 patients with IgAN and 816 controls at the five loci listed in Table 1. The genotype distributions we observed in controls did not differ from the expected frequency under the assumption of Hardy-Weinberg equilibrium (data not shown). A significant association to IgAN was observed at the *DRA* locus, but no association was found at the remaining four loci (Table 1).

In view of the strong association found at the *DRA* locus, we genotyped six SNPs present in the *HLA-DRA* gene (Fig. 2). The most significant difference in genotype distribution between patients with IgAN and controls was observed at the DRA SNP-5 locus (Table 2). Homozygosity for major alleles was significantly more common in IgAN patients than in controls ($\chi^2 = 22.87$, $P = 0.000001$). The OR for patients with IgAN versus controls was 1.91 (95% CI 1.46–2.49) for homozygotes of the DRA SNP-5 major allele versus others. One of the three SNPs for which we found positive associations would alter an amino acid sequence: DRA SNP-6, which showed complete LD to DRA SNP-2, would substitute valine for leucine at codon 222 of the *HLA-DRA* gene ($\chi^2 = 19.96$, $P = 0.00004$). The OR for patients with IgAN versus controls was 1.77 (95% CI 1.36–2.31) for homozygotes of the DRA SNP-6 major allele versus others. In contrast, no significant differences were observed for DRA SNP-3 or DRA SNP-4.

Distribution of *HLA-DRB1* alleles

Because the HLA-DRB region lies in close vicinity to *DRA*, we also examined the relationship between the DRB region and SNPs for susceptibility to IgAN. Because *DRB1* is highly polymorphic, we determined the genotypes of 82 IgAN patients and 253 controls by direct DNA sequencing. As shown in Table 3, the frequency of DRB1*04 tends to be higher in patients than in controls ($P = 0.034$), but the association of the *DRB1* gene to IgAN was less significant than that of the *DRA* gene.

Discussion

We have examined the extent and strength of LD within the class II locus of MHC in a Japanese population sample.

Table 1. Genotype frequencies and association tests of SNPs in the class II region (313 cases of IgAN vs 816 controls)

	DOA	*DMB*	*DQB2*	*DRA*	*TSBP*
SNP information					
Contig number	NT_007592.8	NT_007592.8	NT_007592.8	NT_007592.8	NT_007592.8
Location	15399187	15328808	15151100	14860033	14783966
Genetic variation	T>C	C>A	A>G	C>T	C>T
IgAN					
Major allele	0.61	0.45	0.68	0.66	0.65
Minor allele	0.39	0.55	0.32	0.34	0.35
Total	1.00	1.00	1.00	1.00	1.00
Major homozygous	0.36	0.23	0.49	0.46	0.44
Heterozygous	0.49	0.45	0.37	0.39	0.42
Minor homozygous	0.15	0.32	0.14	0.15	0.14
Total	1.00	1.00	1.00	1.00	1.00
Control					
Major allele	0.64	0.51	0.68	0.55	0.61
Minor allele	0.36	0.49	0.32	0.45	0.39
Total	1.00	1.00	1.00	1.00	1.00
Major homozygous	0.41	0.26	0.46	0.31	0.37
Heterozygous	0.45	0.50	0.44	0.48	0.48
Minor homozygous	0.14	0.24	0.10	0.21	0.15
Total	1.00	1.00	1.00	1.00	1.00
χ^2 [*P*]					
Genotype frequency (2 × 3 table)	2.32 [0.3]	7.37 [0.02]	6.52 [0.03]	23.04 [0.000009]	5.05 [0.08]
Allele frequency (major vs minor)	1.77 [0.1]	5.46 [0.01]	0.06 [0.8]	19.82 [0.000008]	3.64 [0.05]
Major homozygous vs others	2.32 [0.1]	1.13 [0.2]	0.79 [0.3]	22.87 [0.000001]	5.03 [0.02]
Minor homozygous vs others	0.23 [0.6]	7.35 [0.006]	3.86 [0.04]	4.37 [0.03]	0.36 [0.5]

SNP, Single-nucleotide polymorphism

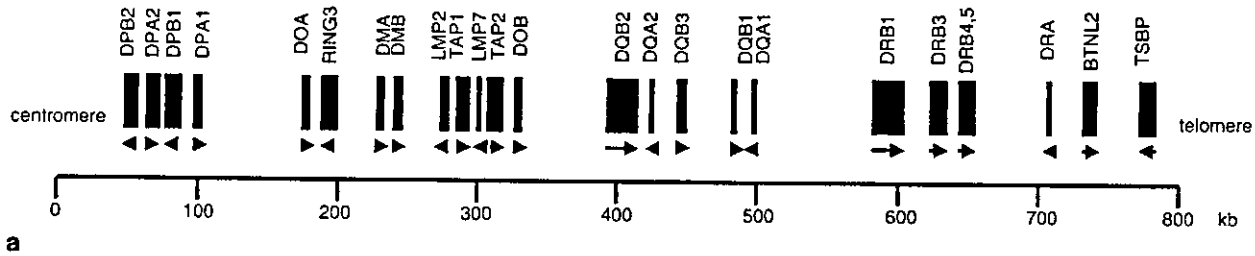

a

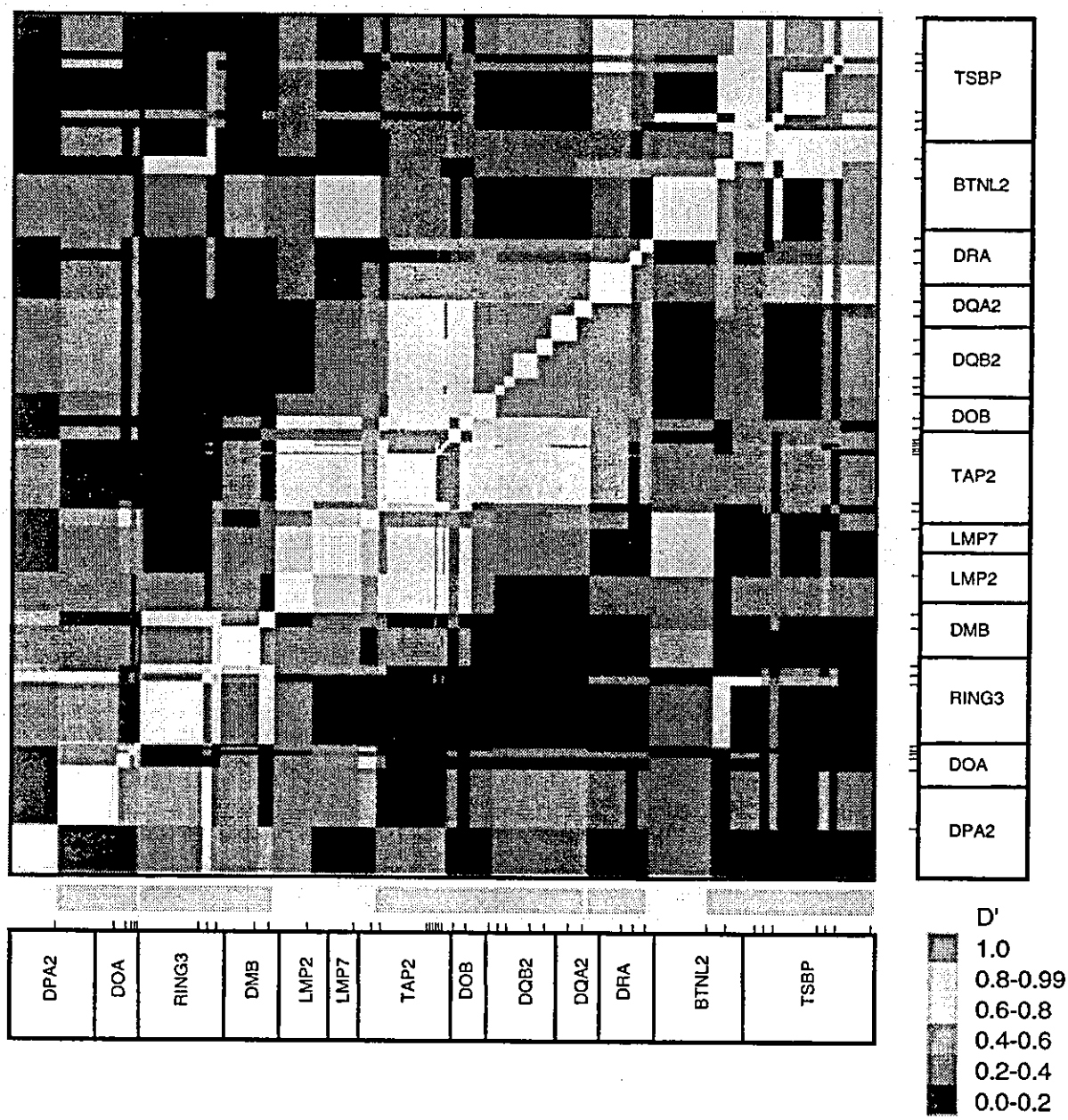

b

Fig. 1. **a** The genomic region extending from *DPB2* to *TSBP* on human chromosome 6p21.3. **b** Distribution of linkage disequilibrium (LD) in the class II region, adjusted for physical distance. Single-nucleotide polymorphism (SNP) sites are indicated by *tick marks* at their locations in the respective genes. Domains showing strong LD are indicated *below* the chart in *light crimson*

Table 2. Genotype data and association tests of SNPs on the *HLA-DRA* gene

	DRA SNP-1[a]	DRA SNP-2	DRA SNP-3	DRA SNP-4	DRA SNP-5	DRA SNP-6
SNP information						
Location	Exon 1 (5'UTR)	Exon 3	Intron 3	Intron 3	Intron 3	Exon 4
Position	−19	402	+64	+133	+280	724
Genetic variation	C/A	C>A	C>T	T>G	C>T	G>T
Substitution		Ile 134 Ile				Val 222 Leu
IgAN						
Major allele [%]		434 [69.3]	515 [82.3]	553 [88.3]	411 [65.7]	434 [69.3]
Minor allele [%]		192 [30.7]	111 [17.7]	73 [11.7]	215 [34.3]	192 [30.7]
Total		626 [100.0]	626 [100.0]	626 [100.0]	626 [100.0]	626 [100.0]
Major homozygous [%]		165 [52.7]	217 [69.3]	249 [79.5]	145 [46.3]	165 [52.7]
Heterozygous [%]		104 [33.2]	81 [25.9]	55 [17.6]	121 [38.7]	104 [33.2]
Minor homozygous [%]		44 [14.1]	15 [4.8]	9 [2.9]	47 [15.0]	44 [14.1]
Total		313 [100.0]	313 [100.0]	313 [100.0]	313 [100.0]	313 [100.0]
Control						
Major allele [%]		1009 [61.8]	1323 [81.1]	1436 [88.0]	903 [55.3]	1009 [61.8]
Minor allele [%]		623 [38.2]	309 [18.9]	196 [12.0]	729 [44.7]	623 [38.2]
Total		1632 [100.0]	1632 [100.0]	1632 [100.0]	1632 [100.0]	1632 [100.0]
Major homozygous [%]		315 [38.6]	537 [65.8]	634 [77.7]	254 [31.1]	315 [38.6]
Heterozygous [%]		379 [46.4]	249 [30.5]	168 [20.6]	395 [48.4]	379 [46.4]
Minor homozygous [%]		122 [15.0]	30 [3.7]	14 [1.7]	167 [20.5]	122 [15.0]
Total		816 [100.0]	816 [100.0]	816 [100.0]	816 [100.0]	816 [100.0]
χ^2 [*P*]						
Genotype frequency (2 × 3 table)		19.96 [0.00004]	2.79 [0.2]	2.64 [0.2]	23.04 [0.000009]	19.96 [0.00004]
Allele frequency (major vs minor)		11.04 [0.0008]	0.43 [0.5]	0.05 [0.8]	19.82 [0.000008]	11.04 [0.0008]
Major homozygous vs others		18.44 [0.00001]	1.26 [0.2]	0.46 [0.4]	22.87 [0.000001]	18.44 [0.00001]
Minor homozygous vs others		0.14 [0.7]	0.74 [0.3]	1.52 [0.2]	4.37 [0.03]	0.14 [0.7]
Odds ratio [95% CI]						
Major homozygous vs heterozygous		1.91 [1.43~2.54]	1.24 [0.92~1.67]	1.20 [0.86~1.68]	1.86 [1.40~2.49]	1.91 [1.43~2.54]
Major homozygous vs others		1.77 [1.36~2.31]	1.17 [0.89~1.55]	1.12 [0.81~1.54]	1.91 [1.46~2.49]	1.77 [1.36~2.31]
Major homozygous vs minor homozygous		1.45 [0.98~2.15]	0.81 [0.43~1.53]	0.61 [0.26~1.43]	2.03 [1.38~2.97]	1.45 [0.98~2.15]

SNP, Single-nucleotide polymorphism; UTR, untranslated region; CI, confidence interval
[a]DRA SNP-1 was not in Hardy-Weinberg equilibrium

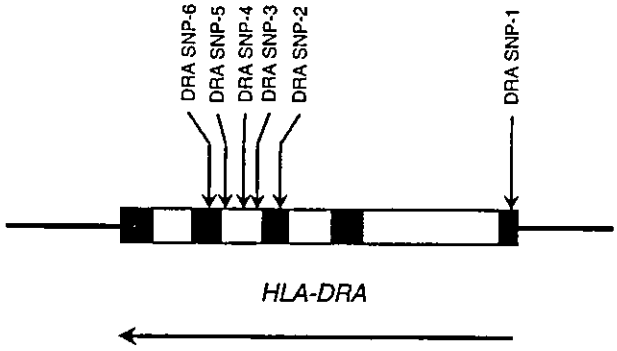

Fig. 2. Location of SNPs in the *HLA-DRA* gene

Table 3. Gene frequencies (%) of *HLA-DRB1* alleles in patients with IgAN and controls

	Group	
DRB1 allele	IgAN (n = 82) 164 alleles	Controls (n = 253) 506 alleles
*01	3.1	5.7
*15	15.2	18.4
*04	26.2†	18.4
*11	2.4	3.4
*12	3.1	4.7
*13	7.3	8.5
*14	13.4	11.5
*07	0.6	0.4
*08	11.0	12.1
*09	17.1	14.8
*10	0.6	1.4

†P = 0.034

Many factors influence the recombination rate and extent of LD, but a remarkable similarity of LD patterns in the MHC region has been observed in populations whose genetic and demographic histories are vastly different (Zavattari et al. 2000). The distribution of crossover events in the class II region tends to cluster in three hot spots, namely, between *DQB1* and *DQB3*, between *RING3* and *DOA*, and in a region within the *TAP2* gene (Zavattari et al. 2000). The LD blocks in our map were separated by corresponding intervals, defined as *DRA* and *DQA2*, *RING3* and *DOA*, and *TAP2* and *DMB*, indicating consistency with other studies (Jeffreys et al. 2001).

LD is a situation in which two closely located polymorphisms show association with each other. LD enables us to use an allele of one SNP to predict an allele of another (nearby) polymorphism. Any potential instance of LD between an SNP and a disease-causing, functional polymorphism (which might also be an SNP) is the basis for whole-genome association studies designed to detect genes involved in complex diseases (Remm and Metspalu 2002).

We demonstrate that the frequencies of DRB1*04 was increased in patients with IgAN, consistent with other previous reports that HLA-DR4 was associated with IgAN in a Japanese population ($P < 0.04$), although the reported P value was not significantly small (Hiki et al. 1982; Kashiwabara et al. 1982). Moreover, the apparent association between *HLA-DRA* alleles and IgAN has not been clarified in the Japanese or any other ethnic group; we have demonstrated here for the first time a significant association of three SNPs in the *HLA-DRA* gene with IgAN. However, because the *DQA1* and *DQB1* loci, which lie within the same LD domain, are highly polymorphic and remain untyped, we cannot exclude the possibility of an association of either or both of these genes with susceptibility to IgAN.

The class II region of the MHC contains a number of interesting candidates for susceptibility to a variety of diseases because of their polymorphic features and the antigenicity of their products. Strong associations exist between products of the polymorphic HLA-DR alleles and certain autoimmune diseases because HLA-DR molecules are of great importance in the selection and activation of CD4-positive T cells that regulate immune responses against protein antigens (Vyse and Todd 1996). However, the pathophysiology of these autoimmune disorders is not completely understood.

Class II molecules are composed of an alpha chain that is noncovalently associated with a beta chain encoded by the A and B gene loci, respectively, in MHC, and are expressed primarily on antigen-processing cells such as dendritic cells, B lymphocytes, and macrophages. The DR molecule consists a single alpha chain encoded by the *DRA* gene and four species of beta chain encoded by the *DRB1*, *DRB3*, *DRB4*, and *DRB5* genes. For Class II, both the A and B genes contribute to variable α-1 and β-1 domains that form a peptide-binding cleft (Williams 2001). The SNPs for which we found positive association with IgAN are not located in this variable α-1 domain. However, because the amino-acid substitution caused by the DRA SNP-6 occurs in the intracellular domain of the DRA molecule, it may affect the structures of peptides bound to HLA class II antigens.

The fundamental role of class II molecules is to bind to self and nonself peptides and transport them to the plasma membrane of cells for recognition by the T-cell antigen receptor. DRA SNP-6 may bring about individual differences in immune responses by influencing signals for alternative pathways involving internalization of HLA-DR molecules (Stern et al. 1994; Pinet et al. 1995). It is well known that, in autoimmune diseases, the activation of autoreactive CD4-positive T cells, which are inactivated under normal conditions, is considered to be a crucial step in the development of disease. Because the IgA antibody response is T-cell dependent, the MHC class II products encoded by DR genes might play a crucial role in the presentation of processed antigen to specific T cells (Hsu et al. 2000). However, the exact mechanism by which the DRA molecule contributes to the development of IgAN remains to be determined.

Acknowledgments We gratefully acknowledge assistance from Kyoko Kobayashi, Susumu Saito, Akihiro Sekine, and technicians at the SNP Research Center, The Institute of Physical and Chemical Research (RIKEN). This work was supported in part by a "Research for the

Future" Program Grant of The Japan Society for the Promotion of Science to Y.N.

References

Devlin B, Risch N (1995) A comparison of linkage disequilibrium measures for fine-scale mapping. Genomics 29:311–322

Floege J, Feehally J (2000) IgA nephropathy: recent developments. J Am Soc Nephrol 11:2395–2403

Galla JH (1995) IgA nephropathy. Kidney Int 47:377–387

Galla JH (2001) Molecular genetics in IgA nephropathy. Nephron 88:107–112

Hiki Y, Kobayashi Y, Tateno S, Sada M, Kashiwagi N (1982) Strong association of HLA-DR4 with benign IgA nephropathy. Nephron 32:222–226

Hsu SIH, Ramirez SB, Winn MP, Bonventre JV, Owen WF (2000) Evidence for genetic factors in the development and progression of IgA nephropathy. Kidney Int 57:1818–1835

Jeffreys AJ, Kauppi L, Neumann R (2001) Intensely punctate meiotic recombination in the class II region of the major histocompatibility complex. Nat Genet 29:217–222

Julian BA, Quiggins PA, Thompson JS, Woodford SY, Gleason K, Wyatt RJ (1985) Familial IgA nephropathy. Evidence of an inherited mechanism of disease. N Engl J Med 312:202–208

Kashiwabara H, Shishido H, Tomura S, Tuchida H, Miyajima T (1982) Strong association between IgA nephropathy and HLA-DR4 antigen. Kidney Int 22:377–382

Lander E, Kruglyak L (1995) Genetic dissection of complex traits: guidelines for interpreting and reporting linkage results. Nat Genet 11:241–247

Mein CA, Barratt BJ, Dunn MG, Siegmund T, Smith AN, Esposito L, Nutland S, Stevens HE, Wilson AJ, Phillips MS, Jarvis N, Law S, de Arruda M, Todd JA (2000) Evaluation of single nucleotide polymorphism typing with invader on PCR amplicons and its automation. Genome Res 10:330–343

Moore R (1993) MHC gene polymorphism in primary IgA nephropathy. Kidney Int 43(Suppl 39):S9–S12

Nielsen DM, Ehm MG, Weir BS (1998) Detecting marker-disease association by testing for Hardy-Weinberg disequilibrium at a marker locus. Am J Hum Genet 63:1531–1540

Ohnishi Y, Tanaka T, Yamada R, Suematsu K, Minami M, Fujii K, Hoki N, Kodama K, Nagata S, Hayashi T, Kinoshita N, Sato H, Sato H, Kuzuya T, Takeda H, Hori M, Nakamura Y (2000) Identification of 187 single nucleotide polymorphisms (SNPs) among 41 candidate genes for ischemic heart disease in the Japanese population. Hum Genet 106:288–292

Pinet V, Vergelli M, Martin R, Bakke O, Long EO (1995) Antigen presentation mediated by recycling of surface HLA-DR molecules. Nature 375:603–606

Remm M, Metspalu A (2002) High-density genotyping and linkage disequilibrium in the human genome using chromosome 22 as a model. Curr Opin Chem Biol 6:24–30

Sabatier JC, Genin C, Assenat H, Colon S, Ducret F, Berthoux FC (1979) Mesangial IgA glomerulonephritis in HLA-identical brothers. Clin Nephrol 11:35–38

Schena FP (1995) Immunogenetic aspects of primary IgA nephropathy. Kidney Int 48:1998–2013

Scolari F, Amoroso A, Savoldi S, Mazzola G, Prati E, Valzorio B, Viola BF, Nicola B, Movilli E, Sandrini M, Campanini M, Maiorca R (1999) Familial clustering of IgA nephropathy: further evidence in an Italian population. Am J Kidney Dis 33:857–865

Stern LJ, Brown JH, Jardetzky TS, Gorga JC, Urban RG, Strominger JL, Wiley DC (1994) Crystal structure of the human class II MHC protein HLA-DR1 complexed with an influenza virus peptide. Nature 368:215–221

Takei T, Iida A, Nitta K, Tanaka T, Ohnishi Y, Yamada R, Maeda S, Tsunoda T, Takeoka S, Ito K, Honda K, Uchida K, Tsuchiya K, Suzuki Y, Fujioka T, Ujiie T, Nagane Y, Miyano S, Narita I, Gejyo F, Nihei H, Nakamura Y (2002) Association between single-nucleotide polymorphisms in selectin genes and immunoglobulin A nephropathy. Am J Hum Genet 70:781–786

Tolkoff-Rubin NE, Cosimi AB, Fuller T, Rubin RH, Colvin RB (1978) IgA nephropathy in HLA-identical siblings. Transplantation 26:430–433

Usami T, Koyama K, Takeuchi O, Morozumi K, Kimura G (2000) Regional variations in the incidence of end-stage renal failure in Japan. JAMA 284:2622–2624

Vyse TJ, Todd JA (1996) Genetic analysis of autoimmune disease. Cell 85:311–318

Williams TM (2001) Human leukocyte antigen gene polymorphism and the histocompatibility laboratory. J Mol Diagn 3:98–104

Zavattari P, Deidda E, Whalen M, Lampis R, Mulargia A, Loddo M, Eaves I, Mastio G, Todd JA, Cucca F (2000) Major factors influencing linkage disequilibrium by analysis of different chromosome regions in distinct populations: demography, chromosome recombination frequency and selection. Hum Mol Genet 9:2947–2957

Kidney International, Vol. 61 (2002), pp. 1577–1587

Gene expression profile of renal proximal tubules regulated by proteinuria

Hideaki Nakajima, Masaru Takenaka, Jun-Ya Kaimori, Yasuyuki Nagasawa, Atsushi Kosugi, Shouko Kawamoto, Enyu Imai, Masatsugu Hori, and Kousaku Okubo

Department of Internal Medicine and Therapeutics, Osaka University Graduate School of Medicine, School of Allied Health Sciences, and Institute for Molecular and Cellular Biology, Osaka University, Osaka, Japan

Gene expression profile of renal proximal tubules regulated by proteinuria.

Background. Proximal tubules activated by reabsorption of protein are thought to play significant roles in the progression of kidney diseases. Thus, identification of genes related to proteinuria should provide insights into the pathological process of tubulointerstitial fibrosis.

Method. Gene expression profiles were constructed by means of direct sequencing procedures to identify genes induced in the mouse kidney proximal tubules (PT) exposed to proteinuria.

Results. By comparing the gene expression of control PT to that of disease model PT, the abundantly expressed genes in control PT were down-regulated presumably because of potentially toxic effects of proteinuria. From the more than 1000 up-regulated genes, an immunity related gene, thymic shared antigen-1 (TSA-1), and a novel gene, GS188, were selected for further characterization. The increased expression of TSA-1, a member of the Ly-6 family, and of GS188 in response to proteinuria was confirmed by Northern analysis, immunohistochemistry, in situ hybridization and laser microdissection along with real-time PCR analysis. Full length cloning of GS188 identified it as a family member of LR8 that was reported to express predominantly in fibroblasts.

Conclusions. The gene expression profiles showed that the expression patterns in PT were changed dramatically by proteinuria. The profiles include novel genes that should be further characterized to aid the understanding of the pathophysiology of progressive kidney diseases.

Recent studies have shown that abundant urinary proteins filtered through the glomerular capillaries induce intrinsic renal toxicity [1–3]. In chronic nephropathies, proteinuria is reportedly one of the best predictors, which is independent of mean arterial blood pressure, for disease progression toward end-stage renal failure [4, 5]. Microalbuminuria, which features reduced protein (30 to 300 mg/24 h) and only albumin in urine, is known as an important early sign of diabetic nephropathy [6, 7] and of progressive renal function loss in a non-diabetic population [8]. In experimental in vivo models of proteinuria, repeated intravenous injections of albumin have been shown to increase permeability of the glomerular barrier and cause proteinuria [9, 10]. These events are followed by tubular changes accompanying infiltration of macrophages and T lymphocytes into the kidney [9]. Consequently, interstitial inflammation could trigger fibroblast proliferation and accumulation of extracellular matrix proteins, which may facilitate the progression of renal disease. Several factors, including osteopontin [11], intercellular adhesion molecule-1 (ICAM-1), vascular cellular adhesion molecule-1 (VCAM-1), transforming growth factor-β1 (TGF-β1) [12] and monocyte chemoattractant protein-1 (MCP-1) [13], have been shown to play important roles in causing renal damage.

In vitro experiments, proximal tubular cells (PT) with protein overload were found to activate the transcription of a number of genes encoding vasoactive and inflammatory molecules that have potentially toxic effects on the kidney [14]. For instance, protein overload stimulated RANTES (regulated upon activation, normal T cell expressed and secreted) production by PT that is dependent on nuclear factor-κB (NF-κB) activation [15]. RANTES has a potent chemotactic effect on monocytes and T lymphocytes [16]. Moreover, expression of major histocompatibility complex (MHC) class I, II and B7-1 (CD80) has been found on murine renal tubular epithelial cells [17, 18]. Engagement of the T cell receptor with both MHC/Ag and a second signal is needed for the complete activation of the T cell, while the CD28/B7 receptor/ligand system represents one of the dominant co-stimulatory pathways of T lymphocytes. Thus, expressions of MHC class I, II and B7-1 on tubular epithelial cells raise the possibility of direct interaction between

Key words: proteinuria, proximal tubule, gene expression, thymic shared antigen-1, Ly-6, LR8, laser microdissection, tubulointerstitial fibrosis, progressive renal disease.

Received for publication September 6, 2001
and in revised form November 29, 2001
Accepted for publication December 3, 2001

tubular epithelial cells and T cells. These results strongly suggest that proximal tubular cells should be involved in the process of renal damage by proteinuria.

To study changes in the in vivo gene expression in proximal tubular epithelial cells caused by proteinuria, we used expression profiling with the aid of the body map procedure [19, 20]. This method is thought to be useful for the application of functional genomics to the study and identification of genes related to kidney diseases [21–23]. For the study presented here, we constructed an expression profile of the renal PT isolated from the albumin-overloaded proteinuria mouse kidney. It was compared with that of normal mice [22] to detect changes in gene expression in PT caused by proteinuria. This comparison made it clear that abundantly expressed genes in normal PT were mostly down-regulated and over 1000 genes were up-regulated in disease model PT. Consequently, several genes that have not been reported as expressed in normal PT were identified only in disease model PT. Among them, immunity related genes and a novel gene predominantly expressed in disease model PT were selected and further characterized. The cloning of the novel gene termed GS188 showed that this was a family member of LR8 that was thought to be a specific marker of fibroblasts [24]. The data from genome projects allowed us to identify the exon-intron composition of GS188 and establish that the distance between LR8 and the novel gene GS188 is approximately 10 kb on the same chromosome of both human and mouse genomes. All data identified by the profiling procedures are accessible on our Internet web site (http://www.med.osaka-u.ac.jp/pub/medone/kidney/array/index.html).

METHODS

Murine protein-overload model preparation

Proximal tubular cells were isolated from five-week-old C57B/6 male and female mice weighing about 20 g. Experimental mice were intraperitoneally given 10 mg/g wt bovine serum albumin (BSA; CAT# A-7906; Sigma Chemical Company, St. Louis, MO, USA) dissolved in saline for five days during one week. The final dose of 10 mg/g wt was reached by incremental increases in the dose over the first week, beginning with 2.5 mg/g wt. The load of BSA was continued to three weeks. Control mice were treated with saline [25, 26].

Microdissection of mouse proximal tubules

After anesthesia, the mice were sacrificed. The kidneys were flushed with 5 mL of dissection solution (at 4°C, containing 135 mmol/L NaCl, 1 mmol/L Na_2HPO_4, 1.2 mmol/L Na_2SO_4, 1.2 mmol/L $MgSO_4$, 5 mmol/L KCl, 2 mmol/L $CaCl_2$, 5.5 mmol/L glucose, and 5 N-2-hydroxyethylpiperazine -N'-2'-ethanesulfonic acid, pH 7.4). They were then dissected and immersed in RNAlater reagent (Ambion, Austin, TX, USA), followed by transfer to a microdissecting dish and cooling to 4°C. The PT containing S1, S2 and S3 cells were collected from the kidneys by microdissection under a stereoscopic microscope. The total length of the isolated PT was estimated to be approximately 300 mm.

Library construction, sequencing and data analyses

RNA was prepared from the microdissected PT with the TRIzol reagent (Life Technologies, Grand Island, NY, USA) according to the manufacturer's instructions. Construction of the 3'-directed cDNA libraries and transformation into *E. coli* were conducted as described elsewhere [20]. Briefly, cDNA was synthesized by using a pUC19 based vector primer, digested by Mbo I, a dam-methylase-sensitive four-base cutter, circularized, and transformed into *E. coli*. The transformant colonies of 3000 randomly selected clones were cultured in 96-well plates. The inserted cDNAs were amplified with flanking primers and cycle sequenced. The data analysis was performed as previously described [22]. We have characterized two clones (GS6736 and GS188) that were identified abundantly and specifically in the profile of albumin overloaded PT.

Cloning of cDNAs

GS6736 and GS188 were two of the genes that were up-regulated in their gene expression profile as a result of the protein overload. We first assembled selected mouse EST sequences to obtain maximum partial sequences. The resulting mouse cDNA sequences then formed the basis for the design of primers for 5'-RACE reactions in order to extend the cDNA of the whole kidney albumin-overloaded for one week. The primer used for cloning GS6736 was 5'-CCTGGGACCTAAAAGGAGCTG-3' and that for cloning GS188 was 5'-ATCAATGTGGG TGGGTTGTGGAG-3'. The SMART-RACE cDNA amplification kit (Clontech, Palo Alto, CA, USA) was used according to the manufacturer's instructions. Polymerase chain reaction (PCR) products were cloned to a pSTBlue-1 vector (Novagen, WI, USA), and DNA sequencing was performed by using an ABI PRISM™ 310 genetic analyzer (Perkin-Elmer Corporation, Norwalk, CT, USA). To prepare the probe for GAPDH cDNA, PCR reaction was performed according to the method reported by Sabath, Broome and Prystowsky [27]. The sequence was verified by direct amplification of the whole cDNA sequence by reverse transcription (RT)-PCR using a primer pair at the extreme 5'- and 3'-ends of the extended cDNA sequence with mouse kidney mRNA as the template.

Tissue preparation

Kidneys were removed after perfusion with phosphate-buffered saline (PBS) to isolate mRNA for North-

Table 1. Expression profiles in control and disease model proximal tubules, inner medullary collecting ducts, and liver

Up-regulated genes								
GS	Size	cPT	dPT	CD	L	Classification	Acc#	Gene name
261	223	0	15	1	1	Lysozyme-, ubiquitin- and proteasome-related	X82636	Rat mRNA for a fusion protein of ubiquitin and ribosomal protein L40
2053	357	0	10	1	0	Lysozyme-, ubiquitin- and proteasome-related	X65922	Mouse fau
156	324	0	10	2	2	Lysozyme-, ubiquitin- and proteasome-related	X51703	Mouse mRNA for ubiquitin
1672	104	0	6	0	0	Lysozyme-, ubiquitin- and proteasome-related	D21800	Rat mRNA for proteasome subunit RC10-II
646	345	0	5	0	0	Lysozyme-, ubiquitin- and proteasome-related	X53304	Rat mRNA for proteasome subunit RC9
334	130	0	4	0	1	Lysozyme-, ubiquitin- and proteasome-related	M21050	Mouse lysozyme M gene, exon 4
288	190	0	3	0	1	Lysozyme-, ubiquitin- and proteasome-related	U13393	Mouse delta proteasome subunit
184	295	0	3	3	1	Lysozyme-, ubiquitin- and proteasome-related	S40697	Mouse UbC = polyubiquitin
2517	382	0	2	0	0	Lysozyme-, ubiquitin- and proteasome-related	D45250	Rat mRNA for proteasome activator rPA28 subunit beta
2397	136	0	1	0	0	Lysozyme-, ubiquitin- and proteasome-related	L17127	Rat proteasome RN3 subunit
2150	425	0	1	0	0	Lysozyme-, ubiquitin- and proteasome-related	D90258	Rat mRNA for proteasome subunit RC8
298	160	0	1	0	1	Lysozyme-, ubiquitin- and proteasome-related	D45249	Rat mRNA for proteasome activator rPA28 subunit alpha
726	262	0	1	0	0	Lysozyme-, ubiquitin- and proteasome-related	D30804	Rat mRNA for proteasome subunit RC6-1
3169	433	3	12	0	0	Immunity-related	J04806	Mouse osteopontin
995	737	0	11	1	0	Immunity-related	D16432	Mouse CD63 mRNA for murine homologue of CD63/ME491
318	161	0	8	0	1	Immunity-related	X04648	Mouse mRNA for IgGl/IgG2b Fc receptor (FcR)
15096	131	0	5	0	0	Immunity-related	L38444	Mouse (clone U2) T-cell specific protein
1249	517	0	4	0	0	Immunity-related	M18184	Mouse lymphocyte differentiation antigeen (Ly-6.2)
207	263	0	4	0	1	Immunity-related	L07607	Mouse migration inhibitory factor (10K protein)
6736	397	0	3	1	0	Immunity-related	U47737	Mouse thymic shared antigen-1 (TSA-1)
3778	310	0	2	0	0	Immunity-related	AF047015	Ovis aries T cell receptor gammal constant region gene, partial cds
9824	77	0	1	0	0	Immunity-related	V01527	Mouse gene coding for major histocompatibility antigen class II (I-A-beta)
18103	270	0	1	0	0	Immunity-related	M64239	Mouse T-cell receptor alpha/delta chain locus
18235	260	0	1	0	0	Immunity-related	M63725	Mouse binding protein for T-cell receptor (TCR-ATFI)
7358	289	0	1	0	0	Immunity-related	M63284	Mouse IgG receptor gene
3614	114	0	1	1	0	Immunity-related	K02896	Mouse MHC class I H2-L gene (haplotype d)
7585	70	0	1	0	0	Immunity-related	J05020	Mouse mast cell high affinity IgE receptor (Fc-epsilon-RI) gamma subunit
18140	283	0	1	0	0	Immunity-related	AE000665	Mouse TCR beta locus from bases 501860 to 700960 (section 3 of 3) of the complete sequence
15175	275	0	1	0	0	Immunity-related	U00204	Ovis aries MHC class II DRB (Ovar-DRB01) gene, partial cds
16181	265	0	1	0	0	Immunity-related	L32659	Bovine monocyte chemoattractant protein-1 (MCP-1) gene exons 1-3

Down-regulated genes								
GS	Size	cPT	dPT	CD	L	Classification	Acc#	Gene name
4001	251	12	1	1	0	Miscellaneous	D88899	Mouse mRNA for KDAP-1
3991	374	9	1	0	0	Miscellaneous	AF068246	Mouse SA protein
4037	343	3	0	0	0	Transporter	X15684	Mouse mRNA for liver-type glucose transporter protein
4343	71	3	0	0	0	Transporter	U12973	Rat Sprague-Dawley renal osmotic stress-in-duced Na-Cl organic solute cotransporter ROSIT
4340	105	3	0	0	0	Receptor	M94583	Mouse alpha-2 adrenergic receptor gene
4095	391	3	0	0	0	Receptor	D17444	Mouse mRNA for soluble D-factor/LIF receptor

Numbered gene signatures (GS) appearing in disease model proximal tubules (PT) more than those in normal PT are listed in descending order of occurrence in the disease model proximal tubule library. Abbreviations are: cTP, control proximal tubules; dPT, disease model proximal tubules; CD, inner medullary collecting ducts; L, liver, Acc#, accession number. Size is given in base pairs.

ern blot analysis. For the histological analyses, kidneys were removed after perfusion with PBS and then with 4% paraformaldehyde (PFA). Specimens were prepared with the paraffin sectioning method after PFA fixation and used for immunostaining and in situ hybridization.

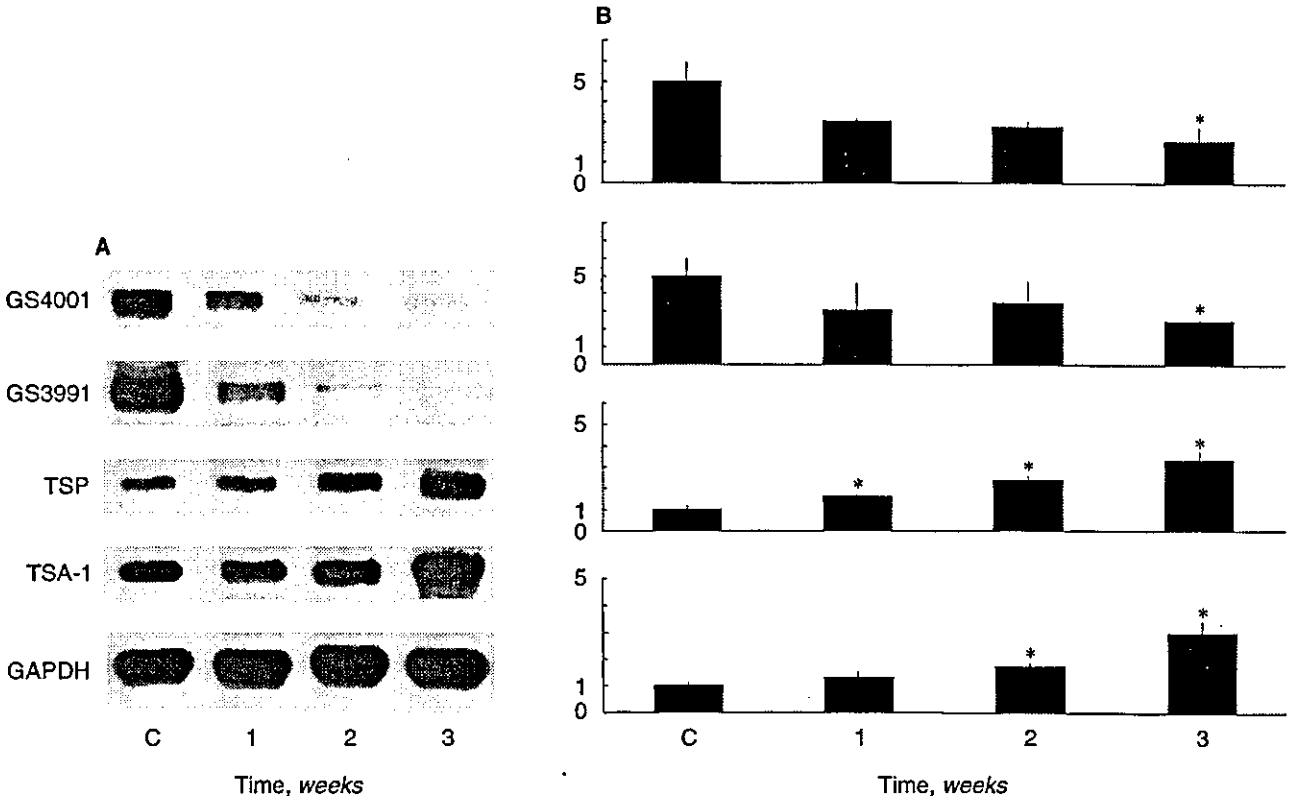

Fig. 1. Northern blot analysis of representative genes in mice treated with protein overload. (*A*) Representative Northern blot data for protein-overloaded mouse kidneys. The genes used as probes in Northern analyses using whole kidney mRNA were GS4001 and GS3991, abundant genes in normal PT, as well as T-cell specific protein (TSP; GS15096) and thymic shared antigen-1 (TSA-1; GS6736), which are genes involved in T-cell activation. Abundantly expressed genes in normal PT were down-regulated, while the expression of TSP and TSA-1 mRNAs was up-regulated during overloading with protein resulting in proteinuria. GAPDH, glyceraldehydes-3-phospate dehydrogenase mRNA. (*B*) The columns on the right show the ratio of each of the mRNA/GAPDH expressions. The points represent the mean of at least three independent experiments (mean ± SE). $^*P < 0.05$ vs. control mice. Shown are C (control) and 1, 2 and 3, weeks (mice with 1, 2 and 3 weeks of BSA administration), respectively.

Northern blot analysis

Total RNA of mouse kidney was extracted with the TRIzol reagent (Life Technologies) according to the manufacturer's instructions. Ten micrograms of each of the RNAs was fractionated on formaldehyde-agarose gels and transferred to nylon membranes (Hybond-N+; Amersham Pharmacia Biotech UK, Buckinghamshire, UK). The membranes were prehybridized for one hour at 65°C with 20 μg/mL of denatured salmon sperm DNA in 0.5% sodium dodecyl sulfate (SDS), 10 × Denhardt's, 5 × standard sodium citrate (SSC) and 50 mmol/L Na phosphate. They were then hybridized overnight with the ^{32}P-labeled probes prepared with the Rediprime II DNA labeling system (Amersham Pharmacia Biotech, Buckinghamshire UK). The membranes were washed twice in 0.1 × SSC with 0.1% SDS for 15 minutes at 60°C and exposed to X-Omat AR films (Eastman Kodak Company, Rochester, NY, USA) with intensifier screens at −80°C for one day. For the cDNA probes, we used the sequences that were obtained by SMART-RACE cDNA amplification (Clontech Laboratories) and confirmed.

Immunohistochemistry

Immunostaining was done for TSA-1 using the monoclonal antibody, PRST1 [28]. Sections were incubated at room temperature for 30 minutes with PRST1, washed twice with PBS and incubated at room temperature for 30 minutes together with the biotinylated secondary antibody. After another washing with PBS, the sections were incubated at room temperature for 30 minutes with VECTASTAIN elite ABC Reagent (Vector Laboratories, Burlingame, CA, USA), and in peroxidase substrate solution for 40 seconds. PT were confirmed by means of the brush borders of PAS staining serial sections (data not shown).

In situ hybridization

Polymerase chain reaction was used to generate the GS188 sense or antisense cRNA probe for the in situ

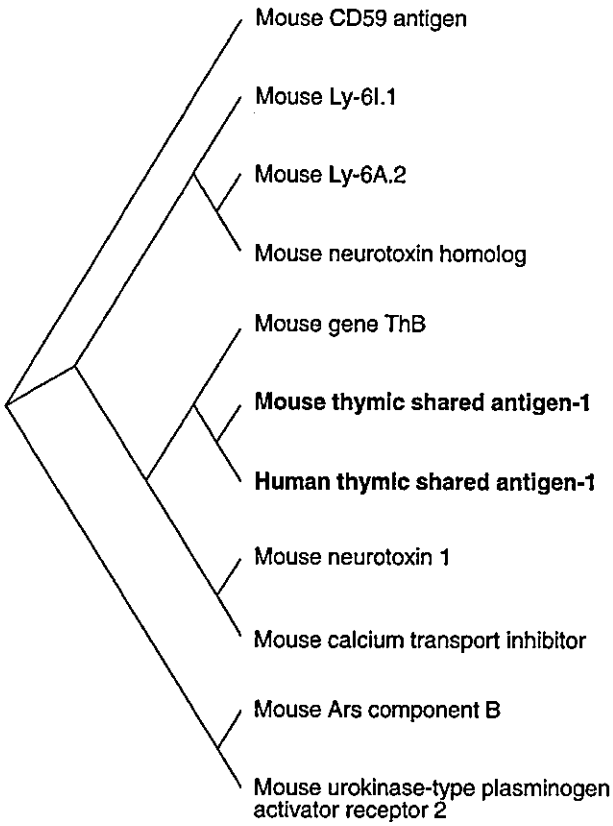

Fig. 2. Phylogenetic analyses of the Ly-6 families including TSA-1. Phylogenetic trees were obtained by means of ClustalW analyses provided by the DDBJ website (http://www.ddbj.nig.ac.jp/Welcome.html), showing that TSA-1 is a member of the Ly-6 family. The accession numbers are: mouse CD59 antigen, NP031678; mouse Ly-6I.1, Q9WU67; mouse Ly-6A.2, AAA39465; mouse neurotoxin homolog, I48639; mouse gene ThB protein, I54553; mouse thymic shared antigen-1, I49013; human thymic shared antigen-1, AAC50616; mouse neurotoxin 1, NP035968; mouse calcium transport inhibitor, Q09098; mouse Ars component B, NP065265; mouse urokinase-type plasminogen activator receptor 2, B41643.

hybridization. The primers for PCR were 5′-TCTGAG TGTGGTTCTGGGTGGAA-3′ and 5′-CCCAGATA CCCAAGAGCATAGCT-3′. The PCR product was subcloned into pSTBlue-1, and the sequence was confirmed to be identical to that of mouse GS188 (data not shown). The subcloned sample was digested by either *Xho* I or *BamHI* as the template of the antisense or sense probe, respectively. The DIG-labeled antisense cRNA probe was produced by using 1 μg of the template and T7 or SP6 RNA polymerase together with the DIG RNA Labeling Mix (Roche Molecular Biochemicals, Mannheim, Germany). In situ hybridization for GS188 was performed with the DNA Nucleic Acid Detection Kit according to the manufacturer's instructions (Roche Molecular Biochemicals).

Tissue sampling by laser microdissection

For laser microdissection, kidneys were removed after perfusion with PBS and then with 99.5% ethanol. They were dehydrated by 30% sucrose/PBS overnight after ethanol fixation, frozen in Tissue-Tek O.C.T. compound (Sakura Company, CA, USA), made into specimens by cryostat and mounted onto 1.35 μm thin polyethylene foils [Laser Pressure Catapulting (LPC) membrane; P.A.L.M. Bernried, Germany] on glass slides. A 0.1% poly-L-lysine solution (Sigma Diagnostics) was used to allow the tissue to tightly adhere onto the membrane. The membrane-mounted specimens were stained rapidly with Carrazzi's Hematoxylin solution (Wako Pure Chemical Industries, Osaka, Japan) for 10 seconds, washed with DEPC-treated water for 10 seconds, dehydrated with 99.5% ethanol and used for laser microdissection with an LM200 Image Archiving Workstation (Arcturus Engineering, CA, USA). Sections were then covered with a transfer film (CapSure TF-100; Arcturus Engineering). The PT were attached to the film by laser beam and collected from the histological sections.

RNA extraction, reverse transcription and real-time PCR

Total RNA was extracted from samples attached to the transfer film by using TRIzol reagent according to the manufacturer's instructions. Extracted RNA was dissolved with 10 μL of DEPC-treated water, and single-strand DNA generated from the RNA by using the SuperScript™ II Reverse Transcriptase (Life Technologies) with random hexamers. The product was used as a template for real-time PCR by using the ABI Prism 7700 Sequence Detection System (Perkin Elmer Applied Biosystems), which is an effective method for reproducible quantitative PCR [29, 30]. The quantitation of mRNA expression of TSA-1 and GS188 was performed with this real-time PCR system according to the manufacturer's instructions and standardization was achieved by using rRNA representation. TaqMan ribosomal RNA Control Reagents (Perkin Elmer Applied Biosystems) were used as internal controls for mRNA expression. The TSA-1 TaqMan probe was 5′-CTGTGGCCAGTT TCATGCCAGGAGAAAGA-3′, the TSA-1 forward primer sequence 5′-GATGTGCTTCTCATGTACCG ATCAG-3′, and its reverse primer sequence 5′-CAGC GGCAGATAACGTGATACAG-3′. The GS188 TaqMan probe was 5′-ACCGCTGTGGCTGCCATCGTT ATT-3′, the GS188 forward primer sequence 5′-CCTG ATGAGGACCCTTCTTGTG-3′, and its reverse primer sequence 5′-CTTTGACAGACATCATCTCCGAGA-3′.

RESULTS AND DISCUSSION

Gene expression profile of proximal tubules isolated from proteinuria model kidney

To study the genes expressed in the renal PT of the albumin-overloaded mice, the expression profile of mRNA isolated from disease model PT was constructed as de-

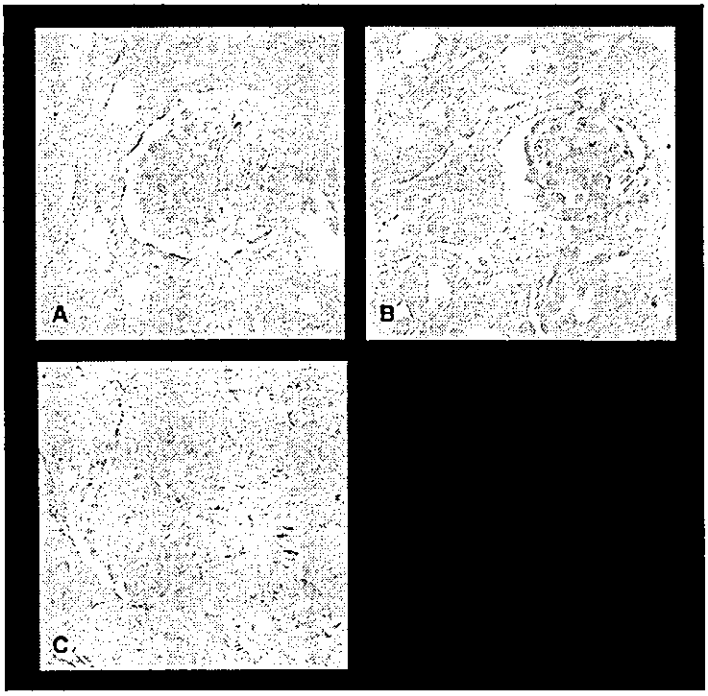

Fig. 3. Immunohistrogical analyses of TSA-1 in the kidney. Immunohistochemical analyses of the kidney were performed by using PRST1, the monoclonal antibody against mouse TSA-1. TSA-1 was expressed on the basolateral side of the tubular epithelium. Shown are (*A*) control, and protein overloading for (*B*) 1 and (*C*) 3 weeks.

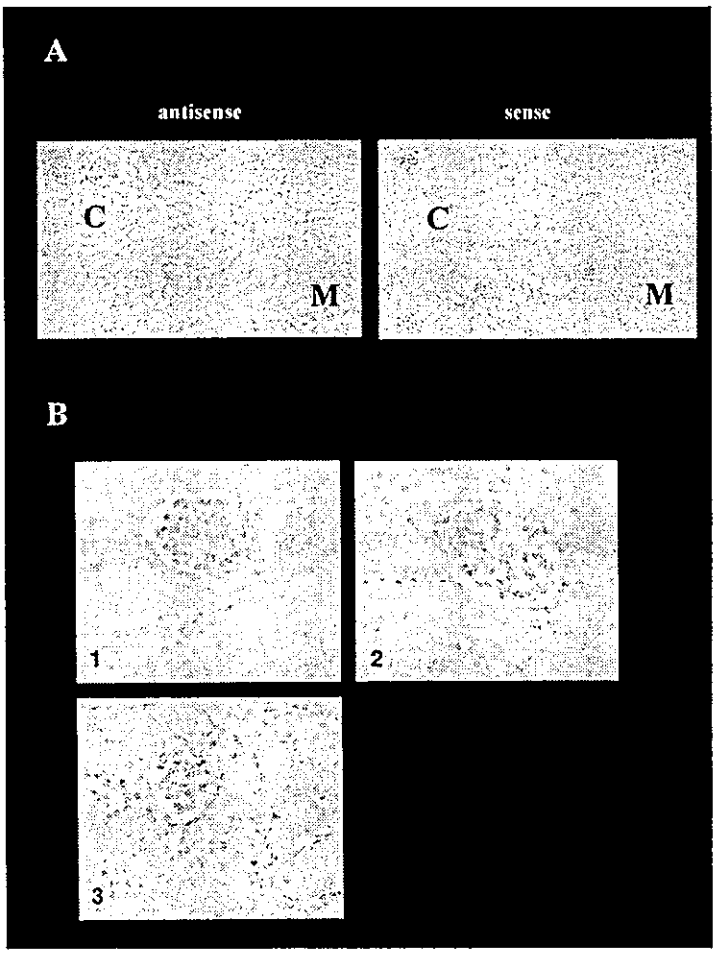

Fig. 7. In situ hybridization of GS188 (*A*) cRNA probe for GS188 was prepared as described in the Methods section. The data obtained with antisense or sense probes are shown (~×100) after 3 weeks of protein-overloaded. Positive signals (dark purple grains) were observed mainly in the (C) cortex rather than (M) the medulla. (*B*) The expression of GS188 in the tubular epithelium was observed mainly in cytoplasmic pattern of the proximal tubules increased during proteinuria exposure of up to 3 weeks, but not in the glomeruli (~×400). Positive signals were shown as dark purple grains. For the visualization of nuclei, a methyl green counter-stain was used. Shown are (1) control, and protein overloading for (2) 1 and (3) 3 weeks.

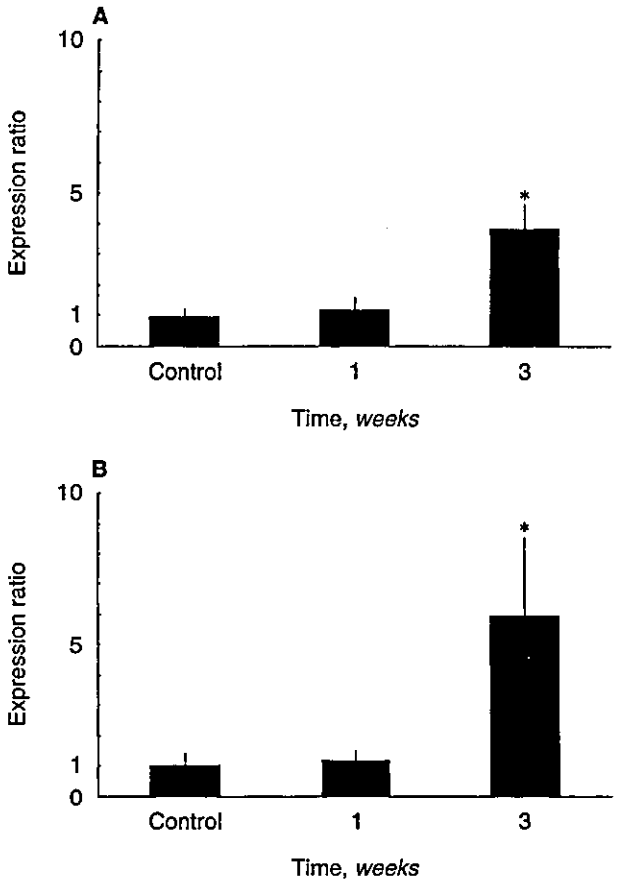

Fig. 4. Quantitative analysis of TSA-1 and GS188 mRNA expression in mouse proximal tubules by laser microdissection as well as with real-time PCR method. The expression of TSA-1 (*A*) and GS188 (*B*) mRNA in PT was quantified by using laser microdissection as well as real-time PCR as described in the **Methods** section. The ratios of TSA-1/rRNA and GS188/rRNA in disease model PT of renal sections from 3-week protein overloaded mice increased by factors of 3.8 ± 0.9 (for TSA-1; $N = 6$, mean ± SE, $P < 0.05$) and 5.9 ± 2.6 (for GS188; $N = 4$, $P < 0.05$) compared with that in control PT, respectively. $^*P < 0.05$ vs. control mice. Shown are controls, and protein overloading for 1 and 3 weeks.

scribed in the **Methods** section. In all, 2006 genes were identified in disease model PT. All data are listed on an Internet document accessible at http://www.med.osaka-u.ac.jp/pub/medone/kidney/array/index.html. Several representative genes regulated by protein overload proteinuria are shown in Table 1. As reported previously [22], GS4001 and GS3991 were expressed abundantly in normal PT. The profile of the disease model PT, however, showed that they were down-regulated. To confirm the data obtained from the expression profiles (Table 1 and our Internet site), Northern analyses using whole kidney mRNA were performed. They demonstrated that the expression of these two abundant genes in normal PT decreased in response to proteinuria after a three-week exposure (Fig. 1). Several other genes that were expressed abundantly in the normal PT profile were down-regulated as well, for example, glucose transporter protein (GS4037) and osmotic stress-induced NaCl organic solute cotransporter (GS4343). Receptor genes such as alpha-2 adrenergic receptor (GS4340) and soluble D-factor/LIF receptor (GS4095) also were down-regulated. These results suggest that the expression of genes abundant in normal PT are reduced because of the potentially toxic effects of proteinuria. On the other hand, over 1000 genes were up-regulated, including various lysozyme-, ubiquitin- and proteasome-related genes such as lysozyme M (GS334), ubiquitin (GS156), fau (GS2053), proteasome subunit RC9 (GS646) and proteasome subunit RC10-II (GS1672). These genes may be involved in absorbed albumin metabolism and/or the degradation pathway. It was of considerable interest in view of the renal damage caused by proteinuria that some immunity-related genes were identified as up-regulated in disease model PT. These genes included osteopontin (GS3169), known as an important regulator of inflammation, CD63 (GS995), which has been associated with cell adhesion, MHC class I (GS3614), MHC class II (GS9824) and MCP-1 (GS16181). These genes are thought to participate in the progression of kidney diseases.

Up-regulation of T-cell specific protein and thymic-shared antigen-1 in protein overload PT

The increased expression of two genes involved in T-cell activation, T-cell specific protein (TSP; GS15096) and thymic shared antigen-1 (TSA-1; GS6736), was confirmed by Northern analyses using mRNA of the whole kidney (Fig. 1). This up-regulation in response to proteinuria has not been previously reported. TSP is a T cell-specific guanine nucleotide triphosphate (GTP)-binding protein and has an important function in T cell development and/or T cell activation [31]. TSA-1 belongs to the Ly-6 molecules and is thought to be a useful marker in early T cell development and T cell activation [28]. The molecules of the Ly-6 family are 10 to 18 kD glycoproteins that link to the cell membrane by means of a GPI anchor. The results of one study indicate that treatment with recombinant interferon-gamma (IFN-γ) markedly increased Ly-6 expression in the kidney, particularly on the luminal side of PT [32]. The function of the Ly-6 family is supposedly that of receptors, such as the urokinase-type plasminogen activator receptor (Fig. 2). The presence of a Ly-6 ligand(s) has been reported on the surface of lymphoid cells [33]. Ly-6 proteins are thought to fulfill some functions in cell signaling and/or cell adhesion processes such as that of the CD59 antigen molecule, which is involved in T-cell activation and cell adhesion [34]. Because of these findings, the Ly-6 family protein TSA-1 has been characterized further. It was expressed on immature thymocytes and thymic epithelial cells [35] as well as in various nonlymphoid tissues [36]. Most of

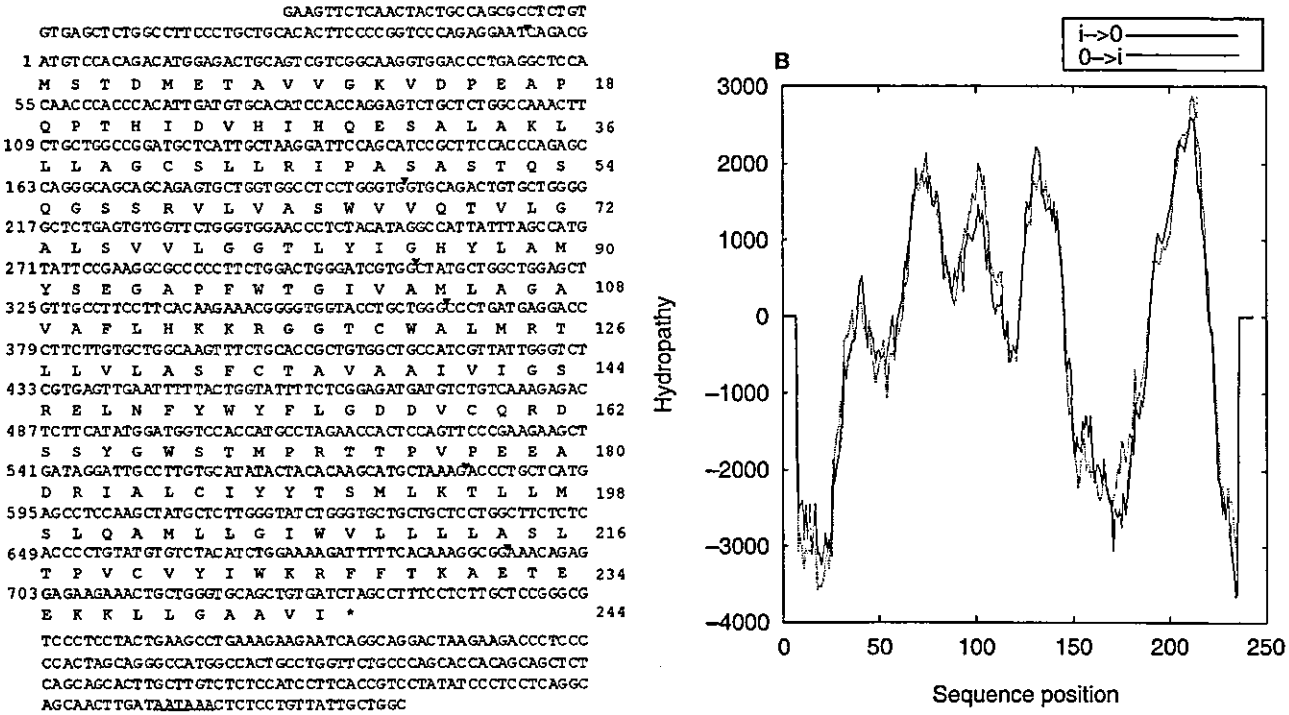

Fig. 5. Nucleotide sequences of GS188 and results of hydropathic analysis. (*A*) GS188 cDNA and its deduced amino acid sequences. GS188 contains a 732-base open reading frame region encoding 244 amino acids shown by a one-letter code. There was an in-frame stop codon in the 5′-untranslated region and a typical polyadenylation signal, AATAAA, which was underlined in the 3′-UTR. The GenBank accession number for the mouse GS188 sequence is AB063313. Closed triangles indicate putative exon-intron boundaries detected as shown in Figure 8. (*B*) Hydropathic analysis predicted by the amino acid sequences of GS188. The hydropathic analysis used the "TMpred" search program (http://www.ch.embnet.org/software/TMPRED_form.html). GS188 was found to contain four strong hydrophobic domains, similar to those of LR8 [24], suggesting that these two gene products have similar structures. FASTA analysis demonstrated 56% similarity between the nucleotide sequences of GS188 and mouse LR8. Solid and dotted line represent inside-to-outside helices and vice versa.

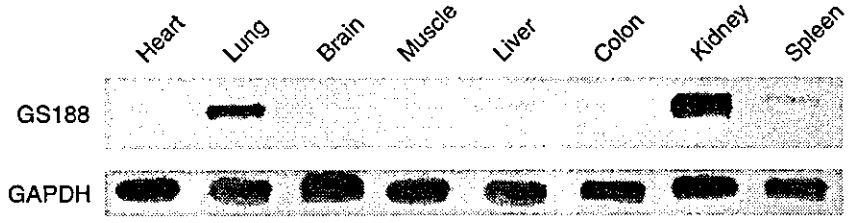

Fig. 6. Northern blot analysis of GS188 using mRNA isolated from various normal tissues. Northern blot analysis revealed that mouse kidney, lung and spleen tissues expressed a prominent transcript. GAPDH is glyceraldehyde-3-phospate dehydrogenase mRNA.

the Ly-6 family proteins are reportedly located on the luminal side of PT [32]. To determine the location of the TSA-1 molecule in the kidney, immunohistochemical analysis using the monoclonal antibody PRST1 [28] was performed. The expression of TSA-1 was clearly identified as a basolateral pattern in the PT after three weeks of protein overload (Fig. 3), while the expression was not detected in control mouse kidney. It should be noted that the basolateral expression of TSA-1 was the same as the expression pattern of MHC classes I and II [18]. The increased expression of TSA-1 mRNA in disease model PT was quantitatively confirmed by laser microdissection method (LMM) along with real-time PCR analysis (Fig. 4A) [37]. We could collect PT with virtually no contamination and quantify mRNA expression by using LMM. The level of TSA-1 mRNA in PT after a three-week protein overload was increased by a factor of 3.8 ± 0.9 compared to that in control PT (Fig. 4A). TSA-1 mRNA expression also increased during albumin overloading at a rate of increase similar to that obtained with Northern analyses using whole kidney mRNA (Fig. 1). Many GPI-anchored proteins have been implicated in the regulation of T cell activation. Kosugi et al provided evidence that the extracellular domain of TSA-1 is physi-

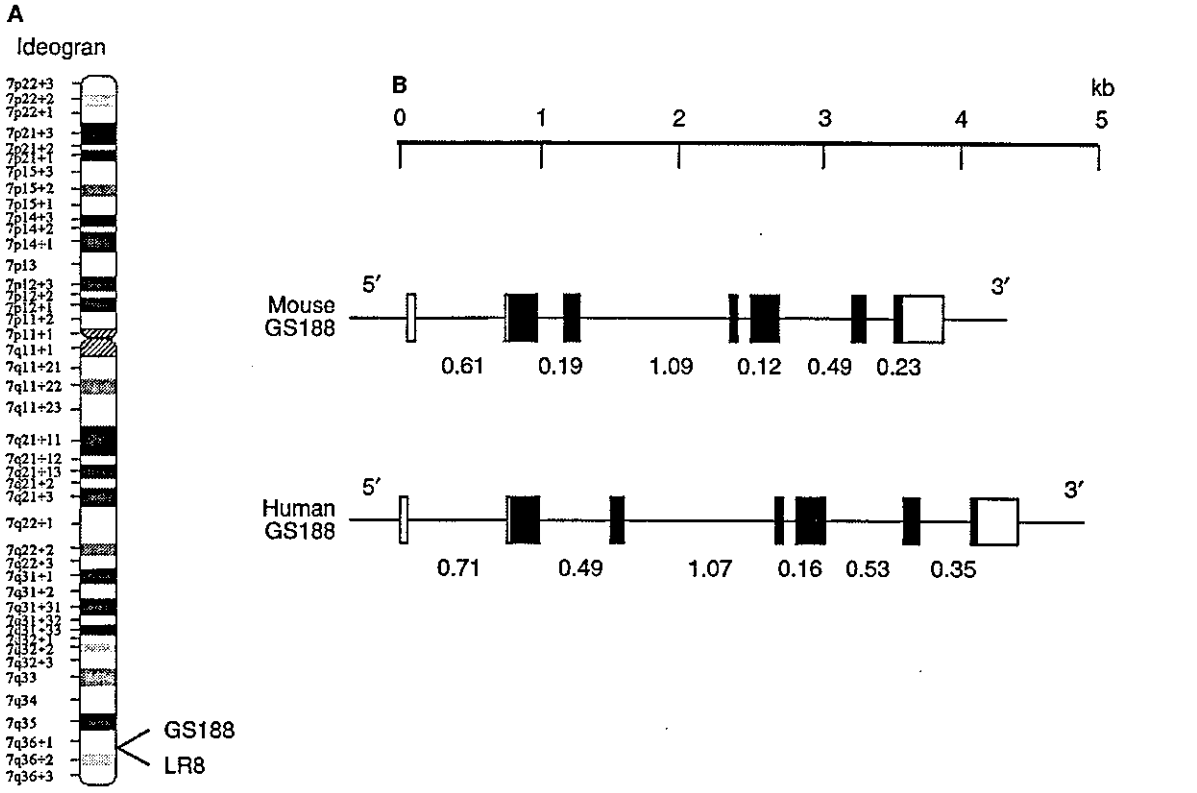

Fig. 8. Location of GS188 and LR8 on the chromosome and the exon-intron composition of mouse and human homologs of GS188 identified by data from the Human and Mouse Genome Projects. (*A*) Location of LR8 and human homolog of GS188 sequences on human chromosome 7. cDNA sequences of GS188 were used for the BLAST search of data of the genome projects. The search revealed that mouse GS188 was located on mouse chromosome 6 (Acc#: AC006949), and the potential human GS188 sequences on human PAC clone RP5-1051J4 from 7q34-q36 (Acc#: AC006479). (*B*) The exon-intron composition of mouse and human homologs of GS188. The open and closed boxes represent non-coding and coding regions, respectively. Detected sequences of the exon-intron boundary are consistent with the "GT-AG" rule (data not shown). Lengths of introns are shown below their gene structure (kb, kilobases).

cally and functionally associated with chains of CD3zeta, a key molecule in TCR signaling pathway [38]. In addition, Classon and Boyd reported that the extracellular domain of TSA-1 binds to a subset of thymocytes, which is consistent with the presence of a TSA-1 ligand on these cells [39]. These findings suggest that TSA-1 is likely to be a cell-surface receptor capable of interacting with a target ligand on the surface of thymocytes. Therefore, it can be hypothesized that the increase in basolateral expression of TSA-1 in the disease model of PT might be involved in the direct interaction between PT and thymocytes.

Up-regulation of an unknown gene, GS188, in the proteinuria model PT

We selected a novel clone, GS188, for further characterization because of its specific expression pattern and up-regulation in response to proteinuria as detected by the analyses using the expression profiles. With the aid of the mouse GS188 cDNA sequence, primers for 5′-RACE reactions were prepared. Several clones for the 5′part of mouse cDNA were obtained, and three independent clones were isolated and sequenced. The full-length mouse GS188 cDNA was about 1.1 kb in size and contained a 732-base open reading frame region encoding 244 amino acids (Fig. 5A). The calculated molecular mass was approximately 26.6 kD, and the putative translational start site was similar to the Kozak consensus sequence [40]. Furthermore, hydropathic analysis of the predicted protein sequence of GS188 revealed that it contained four strong hydrophobic domains (Fig. 5B), suggesting that the putative protein might be a membrane protein. A similarity search of mouse GS188 amino acid sequences was performed by applying the FASTA program to the GenBank. Several similar genes were found listed, for example, human hepatocellular carcinoma-associated antigen 112 (acc#: AF258340, similarity 55.1%), mouse Clast1 (acc#: AB031386, similarity 30.4%), mouse LR8 (acc#: AF115426, similarity 30.4%) and human LR8 (acc#: AF115384, similarity 33.5%). The reported hydropathic analysis of the LR8 amino acid sequence was similar to that of GS188 [24]. Mouse LR8

consists of a 789-base open reading frame region encoding 263 amino acids. The expression of LR8 mRNA is restricted to fibroblasts and reported to be a useful marker of fibroblasts [24]. Northern blot analysis was performed in order to investigate tissue distribution of mouse GS188 mRNA. As shown in Figure 6, mouse kidney, lung and spleen tissues expressed a prominent transcript consistent with the size of the cDNA cloned by us. Lung and spleen were not analyzed with our expression profiling lists, while heart, brain, and skeletal muscle tissues scarcely expressed the mRNA. In situ hybridization was performed to localize mouse GS188 mRNA expression in kidney. Figure 7 shows that its increased expression was seen mainly in PT after a three-week exposure to proteinuria. The expression of GS188 mRNA in disease model PT was quantitatively confirmed by LMM along with real-time PCR analysis as described in the **Methods** section (Fig. 4B) [37]. These procedures detected that GS188 mRNA in PT of the renal section after three weeks of protein overloading had significantly increased by a factor of 5.9 ± 2.6 compared with that in control PT (Fig. 4B). A search of the results of mouse and human genome projects revealed that GS188 was on mouse chromosome 6 (acc#: AC006949) and its potential human counterpart was on human chromosome 7q36 (acc#: AC006479). The *LR8* gene was in the vicinity of the putative GS188 on both the human and mouse chromosome (Fig. 8A). The analysis also demonstrated that the exon-intron composition of human and mouse GS188 gene was virtually identical (Fig. 8B). Two genes were coded in the direction opposite to that of the overlapping 5′ untranslated regions in the putative first introns of the human genome. These findings suggest that GS188 and LR8 are closely related. GS188 and LR8 may have similar functions and may be controlled by similar regulations. The expression of GS188, however, did not seem to be restricted in fibroblasts. Further investigation is needed to identify the precise involvement of GS188 in PT cells.

The gene expression profile showed that the expression pattern in PT was changed dramatically by proteinuria. Not only were genes probably related to process reabsorbed protein identified, but also genes possibly involved in renal damage. The profile indicated that several immunity-related genes are regulated in PT. The increased expression of one of these genes, TSA-1, in PT responding to proteinuria was confirmed by immunohistochemistry and with a recently developed technique, laser-microdissection as well as with the real-time PCR method. Our data suggest that molecules induced by proteinuria may play certain roles in the immune reaction leading to tubulointerstitial damages. The increased expression of a novel gene, GS188, a member of the LR-8 family, may be representative of one of the characteristic changes in the gene expression of PT in this disease model. The information obtained from gene expression profiles can be expected to be useful for the selection and study of transcript in PT involved in the pathophysiology of kidney diseases.

ACKNOWLEDGMENTS

This study was supported in part by a Grant-in-Aid for Scientific research from the ministry of Education, Science, and Culture, Japan. We thank Ms. Naoko Horimoto, Ms. Sonoe Watanabe and Ms. Masako Kishihata for their expert technical support.

Reprint requests to Masaru Takenaka, M.D., Department of Internal Medicine and Therapeutics (Box A8), Osaka University Graduate School of Medicine, 2-2 Yamada-oka, Suita, Osaka, 565-0871, Japan. E-mail: kidney@medone.med.osaka-u.ac.jp

APPENDIX

Abbreviations used in this article are: acc#, accession number; BSA, bovine serum antigen; GPI, glycosyl phosphatidyl inositol; ICAM-1, intercellular adhesion molecule-1; IFN-γ, interferon-gamma; GTP, guanine nucleotide triphosphate; LMM, laser microdissection method; MHC, major histocompatibility complex; PBS, phosphate-buffered saline; PFA, paraformaldehyde; PT, proximal tubule; MCP-1, monocyte chemoattractant protein-1; RANTES, regulated upon activation, normal T cell expressed and secreted; RT-PCR, reverse transcription-polymerase chain reaction; SSC standard sodium citrate; TGF-β1, transforming growth factor beta 1; TSP, T-cell specific protein; TSA-1, thymic shared antigen-1; VCAM-1, vascular cell adhesion molecule-1.

REFERENCES

1. Eddy AA: Experimental insights into the tubulointerstitial disease accompanying primary glomerular lesions. *J Am Soc Nephrol* 5:1273–1287, 1994
2. Remuzzi G: Abnormal protein traffic through the glomerular barrier induces proximal tubular cell dysfunction and causes renal injury. *Curr Opin Nephrol Hypertens* 4:339–342, 1995
3. Remuzzi G, Ruggenenti P, Benigni A: Understanding the nature of renal disease progression. *Kidney Int* 51:2–15, 1997
4. Ruggenenti P, Perna A, Mosconi L, *et al*: Urinary protein excretion rate is the best independent predictor of ESRF in non-diabetic proteinuric chronic nephropathies. "Gruppo Italiano di Studi Epidemiologici in Nefrologia" (GISEN). *Kidney Int* 53:1209–1216, 1998
5. Peterson JC, Adler S, Burkart JM, *et al*: Blood pressure control, proteinuria, and the progression of renal disease. The Modification of Diet in Renal Disease Study. *Ann Intern Med* 123:754–762, 1995
6. Mogensen CE: Microalbuminuria predicts clinical proteinuria and early mortality in maturity-onset diabetes. *N Engl J Med* 310:356–360, 1984
7. Viberti GC, Hill RD, Jarrett RJ, *et al*: Microalbuminuria as a predictor of clinical nephropathy in insulin-dependent diabetes mellitus. *Lancet* 1:1430–1432, 1982
8. Pinto-Sietsma SJ, Janssen WM, Hillege HL, *et al*: Urinary albumin excretion is associated with renal functional abnormalities in a nondiabetic population. *J Am Soc Nephrol* 11:1882–1888, 2000
9. Eddy AA: Interstitial nephritis induced by protein-overload proteinuria. *Am J Pathol* 135:719–733, 1989
10. Remuzzi G, Perna A, Benigni A: Proteins abnormally filtered throughout glomerular capillary have an intrinsic renal toxicity. *Contrib Nephrol* 118:164–172, 1996
11. Abbate M, Zoja C, Corna D, *et al*: In progressive nephropathies, overload of tubular cells with filtered proteins translates glomerular permeability dysfunction into cellular signals of interstitial inflammation. *J Am Soc Nephrol* 9:1213–1224, 1998
12. Eddy AA, Giachelli CM, McCulloch L, *et al*: Renal expression of genes that promote interstitial inflammation and fibrosis in rats with protein-overload proteinuria. *Kidney Int* 47:1546–1557, 1995

13. WANG Y, CHEN J, CHEN L, *et al*: Induction of monocyte chemoattractant protein-1 in proximal tubule cells by urinary protein. *J Am Soc Nephrol* 8:1537–1545, 1997
14. ZOJA C, BENIGNI A, REMUZZI G: Protein overload activates proximal tubular cells to release vasoactive and inflammatory mediators. *Exp Nephrol* 7:420–428, 1999
15. ZOJA C, DONADELLI R, COLLEONI S, *et al*: Protein overload stimulates RANTES production by proximal tubular cells depending on NF-kappa B activation. *Kidney Int* 53:1608–1615, 1998
16. SCHALL TJ, BACON K, TOY KJ, *et al*: Selective attraction of monocytes and T lymphocytes of the memory phenotype by cytokine RANTES. *Nature* 347:669–671, 1990
17. BANU N, MEYERS CM: IFN-gamma and LPS differentially modulate class II MHC and B7–1 expression on murine renal tubular epithelial cells. *Kidney Int* 55:2250–2263, 1999
18. SKOSKIEWICZ MJ, COLVIN RB, SCHNEEBERGER EE, *et al*: Widespread and selective induction of major histocompatibility complex-determined antigens in vivo by gamma interferon. *J Exp Med* 162:1645–1664, 1985
19. OKUBO K, HORI N, MATOBA R, *et al*: A novel system for large-scale sequencing of cDNA by PCR amplification. *DNA Seq* 2:137–144, 1991
20. OKUBO K, HORI N, MATOBA R, *et al*: Large scale cDNA sequencing for analysis of quantitative and qualitative aspects of gene expression. *Nat Genet* 2:173–179, 1992
21. TAKENAKA M, IMAI E, NAGASAWA Y, *et al*: Gene expression profiles of the collecting duct in the mouse renal inner medulla. *Kidney Int* 57:19–24, 2000
22. TAKENAKA M, IMAI E, KANEKO T, *et al*: Isolation of genes identified in mouse renal proximal tubule by comparing different gene expression profiles. *Kidney Int* 53:562–572, 1998
23. TAKENAKA M, IMAI E: Functional genomics in nephrology. *Nephrol Dial Transplant* 14:1–3, 1999
24. LURTON J, ROSE TM, RAGHU G, *et al*: Isolation of a gene product expressed by a subpopulation of human lung fibroblasts by differential display. *Am J Respir Cell Mol Biol* 20:327–331, 1999
25. EDDY AA, KIM H, LOPEZ-GUISA J, *et al*: Interstitial fibrosis in mice with overload proteinuria: Deficiency of TIMP-1 is not protective. *Kidney Int* 58:618–628, 2000
26. NAGASAWA Y, TAKENAKA M, KAIMORI J, *et al*: Rapid and diverse changes of gene expression in the kidneys of protein-overload proteinuria mice detected by microarray analysis. *Nephrol Dial Transplant* 16:923–931, 2001
27. SABATH DE, BROOME HE, PRYSTOWSKY MB: Glyceraldehyde-3-phosphate dehydrogenase mRNA is a major interleukin 2-induced transcript in a cloned T-helper lymphocyte. *Gene* 91:185–191, 1990
28. KOSUGI A, SAITOH S, NARUMIYA S, *et al*: Activation-induced expression of thymic shared antigen-1 on T lymphocytes and its inhibitory role for TCR-mediated IL-2 production. *Int Immunol* 6:1967–1976, 1994
29. FINK L, SEEGER W, ERMERT L, *et al*: Real-time quantitative RT-PCR after laser-assisted cell picking. *Nat Med* 4:1329–1333, 1998
30. GIBSON UE, HEID CA, WILLIAMS PM: A novel method for real time quantitative RT-PCR. *Genome Res* 6:995–1001, 1996
31. CARLOW DA, MARTH J, CLARK-LEWIS I, *et al*: Isolation of a gene encoding a developmentally regulated T cell-specific protein with a guanine nucleotide triphosphate-binding motif. *J Immunol* 154:1724–1734, 1995
32. BLAKE PG, MADRENAS J, HALLORAN PF: Ly-6 in kidney is widely expressed on tubular epithelium and vascular endothelium and is up-regulated by interferon gamma. *J Am Soc Nephrol* 4:1140–1150, 1993
33. ENGLISH A, KOSOY R, PAWLINSKI R, *et al*: A monoclonal antibody against the 66-kDa protein expressed in mouse spleen and thymus inhibits Ly-6A.2-dependent cell-cell adhesion. *J Immunol* 165: 3763–3771, 2000
34. CERNY J, STOCKINGER H, HOREJSI V: Noncovalent associations of T lymphocyte surface proteins. *Eur J Immunol* 26:2335–2343, 1996
35. GODFREY DI, MASCIANTONIO M, TUCEK CL, *et al*: Thymic shared antigen-1. A novel thymocyte marker discriminating immature from mature thymocyte subsets. *J Immunol* 148:2006–2011, 1992
36. CAPONE MC, GORMAN DM, CHING EP, *et al*: Identification through bioinformatics of cDNAs encoding human thymic shared Ag-1/stem cell Ag-2. A new member of the human Ly-6 family. *J Immunol* 157:969–973, 1996
37. NAGASAWA Y, TAKENAKA M, MATSUOKA Y, *et al*: Quantitation of mRNA expression in glomeruli using laser-manipulated microdissection and laser pressure catapulting. *Kidney Int* 57:717–723, 2000
38. KOSUGI A, SAITOH S, NODA S, *et al*: Physical and functional association between thymic shared antigen-1/stem cell antigen-2 and the T cell receptor complex. *J Biol Chem* 273:12301–12306, 1998
39. CLASSON BJ, BOYD RL: Thymic-shared antigen-1 (TSA-1). A lymphostromal cell membrane Ly-6 superfamily molecule with a putative role in cellular adhesion. *Dev Immunol* 6:149–156, 1998
40. KOZAK M: Structural features in eukaryotic mRNAs that modulate the initiation of translation. *J Biol Chem* 266:19867–19870, 1991

Kidney International, Vol. 61 (2002), pp. 1684–1695

Y-27632 prevents tubulointerstitial fibrosis in mouse kidneys with unilateral ureteral obstruction

KATSUYUKI NAGATOYA, TOSHIKI MORIYAMA, NORITAKA KAWADA, MASANOBU TAKEJI, SUSUMU OSETO, TAKAHIRO MUROZONO, AKIO ANDO, ENYU IMAI, and MASATSUGU HORI

Department of Internal Medicine and Therapeutics, Osaka University Graduate School of Medicine, and School of Health and Sport Sciences, Osaka University, Osaka; and Pharmacokinetics Laboratory, Mitsubishi Pharma Corporation, Chiba, Japan

Y-27632 prevents tubulointerstitial fibrosis in mouse kidneys with unilateral ureteral obstruction.

Background. The small GTPase Rho is involved in cell-to-substratum adhesion and cell contraction. These actions of Rho mediated by downstream Rho effectors such as Rho-associated coiled-coil forming protein kinase (ROCK) may be partly responsible for the progression of renal interstitial fibrosis.

Methods. The anti-fibrosis effects of Y-27632, a specific ROCK inhibitor, were studied both in vivo (unilateral ureteral obstruction; UUO) and in vitro. To investigate the therapeutic efficacy of Y-27632 in UUO kidneys, smooth muscle α actin (SMαA) expression, macrophage infiltration and fibrosis in the obstructed kidneys were studied. SMαA, transforming growth factor β (TGF-β), α1 (I) collagen, osteopontin, macrophage chemoattractant peptide-1 (MCP-1), and intercellular adhesion molecule-1 (ICAM-1) gene expression were examined by Northern blotting. To elucidate the mechanism linking the Rho-ROCK pathway with renal fibrosis, the effects of Y-27632 on in vitro cell proliferation and cell migration were studied.

Results. In vivo analysis showed that Y-27632 suppressed SMαA expression, macrophage infiltration and interstitial fibrosis, and that Y-27632 suppressed SMαA, TGF-β and α1 (I) collagen mRNA expression. In vitro analysis showed that Y-27632 did not suppress proliferation of renal fibroblasts but suppressed migration of macrophages.

Conclusions. The Rho-ROCK system may play an important role in the development of tissue fibrosis, and the Rho-ROCK signaling pathway may be a new therapeutic target for preventing interstitial fibrosis in progressive renal disease.

Renal interstitial fibrosis is one of the common histopathological features of progressive renal disease of diverse etiology. Chronic unilateral ureteral obstruction (UUO) is a well-characterized experimental model of renal injury leading to tubulointerstitial fibrosis, pioneered by Klahr and colleagues [1, 2]. UUO is an excellent model of interstitial fibrosis because it is normotensive, non-proteinuric and non-hyperlipidemic, without any apparent immune or toxic renal insult. The molecular and cellular mechanism(s) of interstitial fibrosis in the UUO kidney are beginning to be elucidated. The mechanical disturbance resulting from ureteral ligation (tension stress) [3], hypoxia induced by a marked decline in renal plasma flow [2], up-regulation of monocyte chemoattractant peptide [4], osteopontin [5], intercellular adhesion molecule 1 (ICAM-1) [6] and heat shock protein 47 [7, 8], macrophage influx into the interstitium [4, 9], production of macrophage-derived cytokines, especially transforming growth factor-β (TGF-β) [10, 11], vasoconstrictors such as angiotensin II (Ang II) [12, 13], endothelin [14], and oxidative stress [15, 16] have been shown to play important roles in tubulointerstitial damage in the UUO kidney.

Among more than 50 Ras-related small GTPases, Rho was the first to be identified [17] and has been most extensively studied. Rho is known to function as a molecular switch in various cellular functions including formation of stress fibers and focal adhesions [18], regulation of calcium ion sensitivity in smooth muscle cells [19], regulation of cytokinesis following nuclear division [20] and regulation of G_1 to S cell cycle progression [21]. Although little is known about its mode of action, Rho is activated by stimulants such as lysophosphatidic acid, platelet derived growth factor (PDGF) [18], Ang II [22, 23] and endothelin [24]. Activated Rho binds to specific targets, called effectors, which results in various cellular functions. Among these Rho effectors, Rho-associated coiled-coil forming protein kinase (ROCK) is the best characterized.

As a specific inhibitor of ROCK, Uehata and colleagues reported a synthetic compound named Y-27632 in 1997 [25]. Y-27632 inhibits ROCK by binding to the catalytic site, and its affinities for ROCK as determined by Ki values are 0.22 μmol/L for ROCK-1 and 0.30

Key words: Rho-ROCK pathway, tissue fibrosis, renal fibrosis, progressive renal disease, tubulointerstitial fibrosis, cell proliferation.

Received for publication March 14, 2001
and in revised form December 19, 2001
Accepted for publication December 20, 2001

μmol/L for ROCK-2, which are at least 10- to 20-fold higher than those of two other Rho effector kinases, citron kinase and protein kinase N [26]. Y-27632 is stable in saline at room temperature at least 4 weeks but is metabolized rapidly in vivo. Tissue accumulation has not been reported and oral administration of Y-27632 (100 mg/kg/day) to SD rats for 4 weeks caused no major side effects such as leukopenia (data not shown).

While cellular functions and signal transduction of Rho have been extensively studied, information regarding its in vivo functions is still limited.

In the present study, we hypothesized that the actions of Rho may be partly responsible for the progression of renal interstitial fibrosis and examined this hypothesis by blocking the Rho-ROCK signaling pathway by administration of Y-27632. We demonstrated that tubulointerstitial fibrosis was ameliorated by Y-27632 administration along with the suppression of myofibroblast expansion and macrophage infiltration.

METHODS

In vivo experimental protocol and disease model

This study was designed to determine whether Y-27632 improves tubulointerstitial fibrosis of the kidneys with unilateral ureteral obstruction. Male BDF1 mice (19 to 24 g) were maintained on tap water with sucrose (30% vol/wt) and standard chow (CRF-1; Oriental Yeast, Co. Ltd., Tokyo, Japan). Protocols were approved by Osaka University Medical School Animal Care and Use Committee and were performed according to the Osaka University Medical School Guideline for the Care and Use of Laboratory Animals. Mice were divided into two groups: vehicle control ($N = 10$), and those given Y-27632 ($N = 15$). Y-27632 (a generous gift from Mitsubishi Pharma Corporation, Osaka, Japan) is readily soluble in water, and was added to the drinking water (200 mg/L) from two days before UUO operation until the day of sacrifice. The average water intake of five mice was measured on alternate days, and the inferential dosage of Y-27632 was calculated.

The general procedure of the unilateral ureteral obstruction (UUO) operation was as described previously [8]. For immunohistochemical labeling and RNA extraction, both obstructed and contralateral unobstructed kidneys were harvested from UUO animals at 4 and 10 days after ureteral obstruction ($N = 5$; each group). Midcoronal sections of the kidneys were also taken for immunohistochemical labeling. For the measurement of serum concentration of Y-27632, UUO animals were sacrificed at 7 days after ureteral obstruction ($N = 5$; Y-27632-treated group only).

Cell culture

Primary mouse renal fibroblasts were generated according to the method for human renal fibroblast culture described by Muller and colleagues [27] with slight modifications. The renal cortex was dissected from the kidney, minced and suspended in Dulbecco's modified Eagle's medium (DMEM; Sigma, St. Louis, MO, USA) supplemented with 10% fetal calf serum (FCS; Cell Culture Laboratories, Cleveland, OH, USA). Cells were incubated on collagen-coated plastic dishes (Iwaki, Chiba, Japan) at 37°C in 5% CO_2. After two to three passages, only fibroblasts survived under these culture conditions.

RAW 264.7, a mouse macrophage cell line, were obtained from ATCC (Rockville, MD, USA). Cells were maintained in DMEM supplemented with 10% FCS at 37°C in 5% CO_2.

Measurement of drug concentration

The concentrations of Y-27632 in serum were measured by high-pressure liquid chromatography (HPLC). To serum (0.2 mL) was added 0.2 mL of sodium hydroxide (1 mol/L) followed by extraction with 2.0 mL of chloroform. The organic layer was evaporated at 40°C and was redissolved in 200 μL of mobile phase, and was injected into the L-7000 HPLC system (Hitachi, Tokyo, Japan). Separation was achieved on a reversed-phase column C18 UG-120 n, a Ca pcell pak S-5 (150 mm × 4.6 mm I.D.; Shiseido, Tokyo, Japan) at 40°C. The mobile phase was methanol-20 mmol/L sodium perchlorate adjusted to pH 2.5 with perchloric acid (1:9, vol/vol). The samples were eluted at a constant flow rate of 1.0 mL/min, and the UV detector (L-7400, Hitachi) was set at 270 nm.

Tissue preparation

Kidney sections were fixed in a cold 4% paraformaldehyde (for Masson's trichrome staining and F4/80 detection) or methacarn solution (methanol 60%, chloroform 30%, acetic acid 10%) for smooth muscle α actin (SMαA) detection for 16 to 24 hours, and embedded in paraffin or Tissue-Tec O.C.T. compound (Sakura Finetechnical Co Ltd., Tokyo, Japan). Three-micrometer thick paraffin sections were subjected to Masson's trichrome staining and SMαA detection, and 4-μm thick cryosections were used for F4/80 detection.

Immunohistochemical study

Smooth muscle alpha actin and monocyte/macrophages were identified with mouse anti-SMαA monoclonal antibody (1A4) (EPOS, peroxidase-conjugated; Dako, Denmark) and biotinylated rat anti-mouse F4/80 antigen monoclonal antibody (Serotec Ltd., Oxford, UK), respectively. Immunohistochemical detection of SMαA and F4/80 antigen was performed as previously described [15]. Normal mouse and rat serum were used for negative controls for SMαA and F4/80 staining respectively. No significant staining was observed in the negative controls.

Table 1. Design of the primers

	Sense primer	Antisense primer	Product size *bp*
RhoA	5'-CCAGTTCCCAGAGGTCTATGT-3'	5'-GCGCCAATCCTGTTTGCCATA-3'	375
RhoB	5'-AAGACGTGCCTGCTGATCGTG-3'	5'-CTTGCAGCAGTTGATGCAGCC-3'	531
RhoC	5'-CGACATCGAAGTGGATGGCAA-3'	5'-GGGAAGTCAGAGAATGGGACA-3'	457
TGF-β	5'-AAGACCATCGACATGGAGC-3'	5'-TGTCACAAGAGCAGTGAGCG-3'	580
Osteopontin	5'-ATGAGATTGGCAGTGATTTG-3'	5'-ATGCTCAAGTCTGTGTGTTT-3'	681
MCP-1	5'-AGCCAACTCTCACTGAAGCC-3'	5'-CATTCAAAGGTGCTGAAGACC-3'	256
ICAM-1	5'-TAAGAGGACTCGGTGGATGG-3'	5'-ATGAGGCTCGATTGTTCAGC-3'	550

RNA isolation

RNA of cultured renal fibroblasts, which were treated with Y-27632 (0, 1, 10 or 100 μmol/L), was isolated from subconfluent monolayers in TRIzol reagent (5 mL for a dish; Gibco BRL, Gaithersburg, MD, USA) and for RNA isolation from a whole kidney, tissue was homogenized with a Polytron homogenizer (Kinematica, Switzerland) in TRIzol reagent (4 mL per kidney). Total RNA was prepared by the acid guanidinium isothiocyanate-phenol-chloroform extraction procedure according to the manufacturer's instructions [28].

Reverse transcription

Reverse transcription (RT) was performed as follows: to 0.4 μg of total RNA from whole kidney was added 4 μL first-strand RT buffer (final concentration of 50 mmol/L tris (hydroxymethyl) aminomethane (Tris) hydrochloride, pH 8.3, 75 mmol/L KCl, and 3 mmol/L $MgCl_2$), 2.5 μL H_2O, 0.5 μL RNase inhibitor (55 U), 1 μL of 10 mmol/L deoxynucleotide mixture, 1 μL random primer [0.02 A_{260} absorbance units of hexadeoxyribonucleotide mixture ($p(dN)_6$) per reaction], 2 μL of 0.1 mol/L dithiothreitol (DTT) and 1 μL Moloney murine leukemia virus reverse transcriptase (MMLV transcriptase; Gibco BRL). Reaction tubes were incubated at 30°C for 10 minutes and 42°C for 40 minutes. At the end of the incubation, the reaction was stopped by heating at 95°C for 5 minutes to inactivate the MMLV.

Polymerase chain reaction

Polymerase chain reaction (PCR) was performed as follows: to 1 μL of the RT reaction mixture was added 0.4 μL of 10 μmol/L forward and reverse primer, 2 μL of 10 × buffer (final concentration of 10 mmol/L Tris HCl, pH 8.3, 50 mmol/L KCl, 1.5 mmol/L $MgCl_2$ and 0.001% gelatin), 14.5 μL H_2O, 1.6 μL of 2.5 mmol/L dNTP mix and 0.1 μL of Taq polymerase. The design of RhoA, RhoB and RhoC primers are shown in Table 1. Twenty-five cycles of sequential steps were performed using a terminal cycler; PCR System 9700 (Perkin Elmer, Wellesley, MA, USA) using the following parameters: denaturation at 95°C for one minute, annealing at 58°C for one minute, extension at 72°C for two minutes, followed by a final incubation at 72°C for seven minutes.

Northern blotting

RNA (10 μg from cultured cells and 20 μg from a whole kidney) was size-fractionated on 1% agarose-formaldehyde gels and transferred onto nylon membrane filters (Hybond N+; Amersham, Boston, MA, USA). RNA blots were performed by standard techniques with the ^{32}P-labeled cDNA probes described below. The densities of the bands were quantified with the computing densitometer Image Quant (Molecular Dynamics, Sunnyvale, CA, USA). The following ^{32}P multi-prime-labeled DNA probes for α1 (I) collagen [8], TGF-β, osteopontin, macrophage chemoattractant peptide-1 (MCP-1), ICAM-1, and glyceraldehyde-3-phosphate-dehydrogenase (GAPDH) were prepared using the *redi*prime DNA labeling system (Amersham, Buckinghamshire, UK). The designs of primers of TGF-β, osteopontin, MCP-1 and ICAM-1 are shown in Table 1. Partial cDNAs used as probes were prepared by reverse transcription polymerase chain reaction (RT-PCR) using primers and mouse kidney RNA as templates. cDNA amplified by RT-PCR with these primers was subcloned using a pSTBlue-1 vector kit (Novagen, Milwaukee, WI, USA). Oligonucleotide probe of the mouse SMαA: 5'-CACGAGTAACAAATCAAAGCT TTGGG CAGGAATGATTTGGAAAGGAACTGG AGGCGCTGA TCCACAAAACGTTCACAGTTGT GTGCTA-3' was labeled with T4 polynucleotide kinase using [γ ^{32}P] ATP (3,000 Ci/mmol; Amersham).

Morphometric analysis of the interstitial fibrosis in Masson's trichrome or immunohistochemically stained sections using a computer-aided manipulator

The area of the fibrotic lesion of cortical interstitium was determined on sections stained by Masson's trichrome method to stain the collagen fibers (stained in blue) using computer-aided manipulator program, Macscope (Mitani Corporation, Fukui, Japan), as described previously [8]. The interstitial area positive for immunohistochemical detection was analyzed and quantified as described [16, 29]. The scores of ten fields of each kidney were averaged, and the scores of five separate animals were then averaged.

Cell proliferation assay

Cell proliferation was assessed using the MTT [3,(4, 5-dimethylthiazol-2-yl)2,5-diphenyl-tetrazolium bromide]